Inorg. Chem. **2008**, *47*, 5799−5814

Early Transition Metal Complexes Bearing a C-Capped Tris(phenolate) Ligand Incorporating a Pendant Imine Arm: Synthesis, Structure, and Ethylene Polymerization Behavior

Damien Homden,[†] Carl Redshaw,*[,†] Joseph A. Wright,[†] David L. Hughes,[†] and Mark R. J. Elsegood[‡]

School of Chemical Sciences and Pharmacy, University of East Anglia, Norwich, NR4 7TJ, U.K., and Chemistry Department, Loughborough University, Loughborough, Leicestershire, LE11 3TU, U.K.

Received December 28, 2007

The ligand 3-[2,2′-methylenebis(4,6-di-*tert*-butylphenol)-5-*tert*-butylsalicylidene-(2,6-diisopropyl)phenylimine] (**L**^{1}H$_3$) was reacted with MCl_4 (M = Ti, Zr) or MCl_5 (M = Nb, Ta) to give complexes of the type $[MCl_2(\mathbf{L}^1H_2)_2]$ (M = Ti (**1**); Zr (**2**)), $[NbCl_3(\mathbf{L}^1H)]$ (**3**), or $[TaCl_4(\mathbf{L}^1H_2)]$ (**4**), respectively. Single crystal X-ray diffraction of **1**−**4** revealed common "iminium" species resulting in zwitterionic complexes. Reaction of [V(N*p*-tol)(O*n*-Pr)$_3$] with **L**^{1}H$_3$ afforded $[\{(VNp\text{-tol})(\mathbf{L}^1H)\}_2(\mu\text{-O}n\text{-Pr})_2]$ (**5**), and a second complex $[(VO)_2(\mu\text{-O})(\mathbf{L}^3H)_2]$ (**6**) (**L**^{3}H being derived from 3-[2,2′-methylenebis(4,6-di-*tert*-butylphenol)-5-*tert*-butylsalicylidene-*p*-tolylimine]). The condensation reaction between 3-[2,2′-methylenebis(4,6-di-*tert*-butylphenol)-5-*tert*-butyl-2-hydroxybenzaldehyde] (**L**^{0}H$_3$) and *o*-phenylenediamine (1, 2-diaminobenzene) afforded two products: a pseudo-16-membered hydrogen bonded macrocyclic structure {1,2-bis-3-[2,2′-methylenebis(4,6-di-*tert*-butylphenol)-5-*tert*-butylsalicylidene-benzyldiimine]} (**L**^{5}H$_6$), or the benzimidazolyl bearing ligand (**L**^{6}H$_3$). The reaction of **L**^{5}H$_6$ or **L**^{6}H$_3$ with [VO(O*n*-Pr)$_3$] under varying conditions produced the complexes $[(VO)(\mathbf{L}^5H_4)]$ (**7**), $[(VO)_2(\mathbf{L}^5H)]$ (**8**), or $[VO(\mathbf{L}^6H_2)_2]$ (**9**). **L**^{0}H$_3$ was reacted with a number of anilines to give the proligands {3-[2,2′-methylenebis(4,6-di-*tert*-butylphenol)-5-*tert*-butylsalicylidene-R-imine]}, where R = NC_6H_5 (**L**^{2}H$_3$), NC_6H_4-Me (**L**^{3}H$_3$), and NC_6H_2-Me$_3$ (**L**^{4}H$_3$). Reactions of these ligands with [VO(O*n*-Pr)$_3$] formed bischelating complexes of the form $[(VO)(\mathbf{L}^{2-4}H_2)_2]$ (**10**, **11**, and **12**, respectively). The reaction of **L**^{1}H$_3$ with trimethylaluminum led to a bis-aluminum complex $\{(AlMe_2)[AlMe(NCMe)]\mathbf{L}^1\}$ (**13**). The ability of complexes **1**−**12** to polymerize ethylene in the presence of an organoaluminum cocatalyst was investigated. Procatalysts **1** and **2** were found to produce negligible activities in the presence of dimethylaluminum chloride (DMAC) and the reactivator ethyltrichloroacetate (ETA), whereas **3** and **4** were found to be completely inactive for polymerization using a variety of different organoaluminum cocatalysts. Using the combination of DMAC and ETA, complexes **5**−**12** were found to be highly active catalysts; in all cases, the polymer formed was of high molecular weight linear polyethylene.

Introduction

Chelating aryloxides represent a useful class of ancillary ligand in postmetallocene α-olefin polymerization catalysis.[1] Early breakthroughs included work by Miyatake and Kakugo,[2] who reported good activities for ethylene polymerization when using X_2Tidiphenolate/MAO (X = Cl, *i*-Pr) systems. Extensive alkylation studies followed by Schaverien et al.,[3] using Cl_2Mdiphenolate (or binaptholate) type complexes (M = Ti, Zr) with lithium alkyls or via reaction of the tetrabenzyls $M(CH_2Ph)_4$ with the appropriate biphenol or binapthol. Cationic complexes were available on treatment of the dialkyls with the likes of $B(C_6F_5)_3$. Such species proved useful procatalysts for the cyclotrimerization of

* To whom correspondence should be addressed. E-mail: carl.redshaw@uea.ac.uk.
† University of East Anglia.
‡ Loughborough University.

(1) (a) Britovsek, G. J. P.; Gibson, V. C.; Wass, D. F. *Angew Chem.* **1999**, *111*, 448; *Angew Chem. Int. Ed. Engl.* **1999**, *38*, 428. (b) Gibson, V. C.; Spitzmesser, S. K. *Chem. Rev.* **2003**, *103*, 283. (c) Gibson, V. C.; Marshall, E.L. *Comprehensive Coordination Chemistry II*; McCleverty, J. A., Meyer, T. J., Ward, M. D., Eds; Elsevier: Amsterdam, 2004; p 9.

(2) Miyatake, T.; Mizunuma, K.; Seki, Y.; Kakugo, M. *Makromol. Chem. Rapid Commun.* **1989**, *10*, 349.

(3) Van der Linden, A.; Schaverien, C. J.; Meijboom, N.; Ganter, C.; Orpen, A. G. *J. Am. Chem. Soc.* **1995**, *117*, 3008.

10.1021/ic702506w CCC: $40.75
Published on Web 06/05/2008

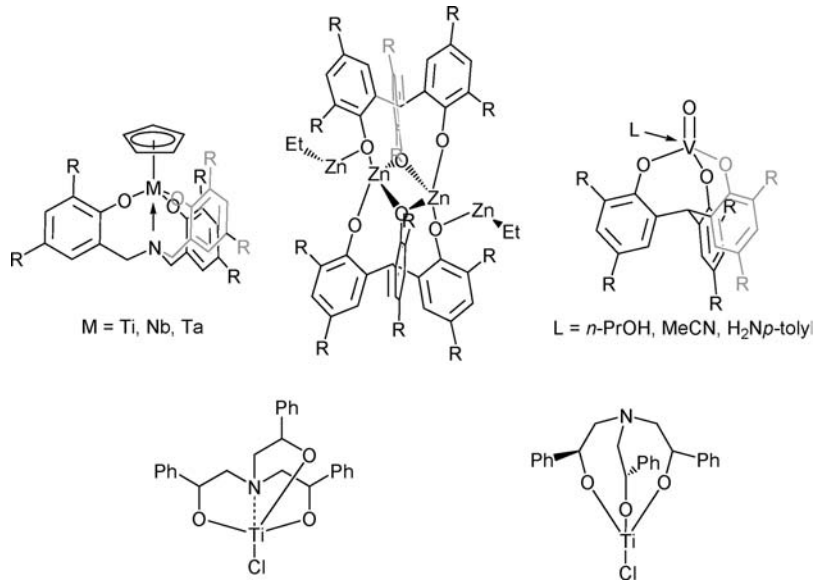

Figure 1. Examples of previously reported capped-metal catalysts.

terminal alkynes, as well as in ethylene and butadiene polymerization. Subsequent work by Okuda et al.,[4] revealed how the nature of the bridging group ($-CH_2-$, $-CH_2CH_2-$, $-S-$, $-SO-$) in diphenolate ancillary ligands could impact upon the resulting catalytic activity in the copolymerization of styrene with ethylene. Other bridging groups, including $-Te-$ and $-SO_2-$, have also been successfully used in ethylene polymerization.[5,6] Such studies no doubt led to the development and use of more functionalized bridges in bis(phenolate)-type ligands, typified by amine bis(phenolate) ligands with a $-CH_2N(R)CH_2-$ bridge (R = $CH_2CH_2CH_3$, $CH_2CH_2NMe_2$) developed by Kol et al. primarily for 1-hexene polymerization.[7] Similar ligands were used more recently by Lorber et al. in ethylene polymerization,[8] as were the phosphorus-bridged ligands $-P(R)-$ (R = Ph, *t*-Bu, C_6H_4-2-CH_2NMe_2, C_6F_5, C_6H_4-2-OMe) developed in the laboratories of the Sumitomo Chemical Co.[9] The coordination chemistry associated with linear triphenols is an emerging area,[10] but their use in catalysis is somewhat limited.[11] Macrocyclic aryloxides, namely, calixarenes, have shown catalytic potential in this area, particularly when they possess dimethylene oxa bridges ($-CH_2-O-CH_2-$).[12] Tripodal ligands, such as tris(3,5-di-*tert*-butyl-2-hydroxyphenyl/benzyl)methane, tris(2-hydroxyphenyl)amine, and 2,2′,2″-nitrilotris(methylene)tris(4,6-dialkylphenol), are useful as trianionic supports for transition metals[13,14] (Figure 1), and work by Nomura et al. (triaryloxoamine), Sundararajan et al. (trialkoxyamine) and by Subhakar (trialkoxyamine) using group IV metals (Ti, Zr) has shown such systems to be useful for the polymerization of 1-alkenes.[15] Bruno, Verkade, Davidson, and Scott have employed such complexes for a variety of other polymerization processes,[16–20] including styrene polymerization, lactide polymerization and the copolymerization of carbon dioxide with epoxides. Half-sandwich titanium complexes incorporating ligands derived from trialkanolamine have been used in the syndiospecific polymerization of styrene.[21]

(4) Sernetz, F. G.; Mülhaupt, R.; Fokken, S.; Okuda, J. *Macromolecules* **1997**, *30*, 1562.
(5) Nakayama, Y.; Watanabe, K.; Ueyama, N.; Nakamura, A.; Harada, A.; Okuda, J. *Organometallics* **2000**, *19*, 2498.
(6) Takaoki, K.; Miyatake, T. *Macromol. Symp.* **2000**, *157*, 251.
(7) (a) Tshuva, E. Y.; Versano, M.; Goldberg, I.; Kol, M.; Weitman, H.; Goldschmidt, Z. *Inorg. Chem. Commun.* **1999**, *2*, 371. (b) Tshuva, E. Y.; Goldberg, I.; Kol, M. *J. Am. Chem. Soc.* **2000**, *122*, 10706. (c) Tshuva, E. Y.; Goldberg, I.; Kol, M.; Weitman, H.; Goldschmidt, Z. *Chem. Commun.* **2000**, 379. (d) Tshuva, E. Y.; Goldberg, I.; Kol, M.; Goldschmidt, Z. *Inorg. Chem. Commun.* **2000**, *3*, 611. (e) Tshuva, E. Y.; Goldberg, I.; Kol, M.; Weitman, H.; Goldschmidt, Z. *Organometallics* **2001**, *20*, 3017. (f) Tshuva, E. Y.; Goldberg, I.; Kol, M.; Weitman, H.; Goldschmidt, *Inorg. Chem.* **2001**, *40*, 4263. (g) Tshuva, E. Y.; Goldberg, I.; Kol, M.; Weitman, H.; Goldschmidt, Z. *Chem. Commun.* **2001**, 2120. (h) Tshuva, E. Y.; Groysman, S.; Goldberg, I.; Kol, M.; Goldschmidt, Z. *Organometallics* **2002**, *21*, 662. (i) Segal, S.; Goldberg, I.; Kol, M. *Organometallics* **2005**, *24*, 200. (j) Gendler, S.; Segal, S.; Goldberg, I.; Goldschmidt, Z.; Kol, M. *Inorg. Chem.* **2006**, *45*, 4783.
(8) Lorber, C.; Wolff, F.; Choukroun, R.; Vendier, L. *Eur. J. Inorg. Chem.* **2005**, 2850.
(9) Hanaoka, H.; Imamoto, Y.; Hino, T.; Kohno, T.; Yanagi, K.; Oda, Y. *J. Polym. Sci., A, Polym. Chem.* **2007**, *45*, 3668.
(10) Kawaguchi, H.; Matsuo, T. *J. Organomet. Chem.* **2004**, *689*, 4228.
(11) Redshaw, C.; Homden, D. M.; Rowan, M. A.; Elsegood, M. R. J. *Inorg. Chim. Acta* **2005**, *358*, 4067.
(12) Redshaw, C.; Rowan, M. A.; Warford, L.; Homden, D. M.; Arbaoui, A.; Elsegood, M. R. J.; Dale, S. H.; Yamato, T.; Casas, C. P.; Matsui, S.; Matsuura, S. *Chem. Eur. J.* **2007**, *13*, 1090.
(13) Kol, M.; Shamis, M.; Goldberg, I.; Goldschmidt, Z.; Alfi, S.; Hayut-Salant, E. *Inorg. Chem. Commun.* **2001**, *4*, 177.
(14) Akagi, F.; Matsuo, T.; Kawaguchi, H. *J. Am. Chem. Soc.* **2005**, *127*, 11936.
(15) (a) Wang, W.; Fujiki, M.; Nomura, K. *Macromol. Rapid Commun.* **2004**, *25*, 504. (b) Sudhakar, P.; Amburose, C. V.; Sundararajan, G.; Nethaji, M. *Organometallics* **2004**, *23*, 4462. (c) Sudhakar, P.; Sundararajan, G. *Macromol. Rapid Commun.* **2005**, *26*, 1854. (d) Sudhakar, P. *J. Polym. Sci. A., Polym. Chem.* **2007**, *45*, 5470.
(16) Bruno, J. W.; Michalczyk, L.; de Gala, S. *Organometallics* **2001**, *20*, 5547.
(17) Kim, Y.; Jnaneshwara, G. K.; Verkade, J. G. *Inorg. Chem.* **2003**, *42*, 1437.
(18) Dinger, M. B.; Scott, M. J. *Inorg. Chem.* **2001**, *40*, 1029.
(19) Chmura, A. J.; Chuck, C. J.; Davidson, M. G.; Jones, M. D.; Lunn, M. D.; Bull, S. D.; Mahon, M. F. *Angew. Chem. Int. Ed.* **2007**, *46*, 2280.
(20) Kim, Y. J.; Kapoor, P. N.; Verkade, J. G. *Inorg. Chem.* **2002**, *41*, 4834.
(21) Kim, Y.; Do, Y. *J. Organomet. Chem.* **2002**, *655*, 186.

As an extension to the "tripod" family, Scott et al. reported a method whereby an aldehyde group was readily appended *ortho* to one of the phenolic groups. Subsequent condensation chemistry proved facile, and new NO_3-type "imine-tripod" ligands bearing an imine arm were readily available; the ligand 3-[2,2′-methylenebis(4,6-di-*tert*-butylphenol)-5-*tert*-butylsalicylidene-benzylimine] (see Scheme 3 in ref 22) has been reported and structurally characterized by Scott et al.[22]

Such imine-tripods can be viewed and, indeed, act as a new class of phenoxyimine ligand. Phenoxyimine ligands have been extensively studied, primarily by Fujita et al. at Mitsui Chemicals,[23,24] and found to be versatile ligands for the production of highly active α-olefin polymerization catalysts based on group IV and V metals. Titanium-based systems, so-called Ti−FI catalysts, bearing two fluorinated phenoxy rings have proved particularly successful in the development of thermally robust, living ethylene and propylene (syndiotactic) polymerization systems. The activity of such species can be controlled by varying the nature of the substituents on the imine nitrogen or indeed on the phenoxy ring. For example, the steric bulk associated with the substituent *ortho* to the phenoxy-oxygen plays a pivotal role in dictating catalytic activity and polymer molecular weight. Activation of bis[*N*-(3-*tert*-butylsalicylidene)-anilinato]zirconium dichloride using *i*-Bu_3Al (30 equiv), followed by subsequent hydrolysis, led to the isolation of phenoxy-amine ligands, leading Fujita et al. to suggest that the active species formed when using *i*-Bu_3Al /$[CPh_3][B(C_6F_5)_4]$ may well contain the reduced form of the ligand, that is, a phenoxy-amine. Interestingly however, NMR/EPR spectroscopy for the pentafluoroaniline/3-*tert*-butylsalicylaldehyde derived Cl_2TiFI system indicated that, in the absence of monomer, reaction with either MAO or $Me_3Al/[CPh_3]$-$[B(C_6F_5)_4]$, deactivation occurred via transfer of the phenoxy-imine ligand to aluminum.[25]

Scheme 1. Representation of Zwitterionic Complexes **1**−**4**

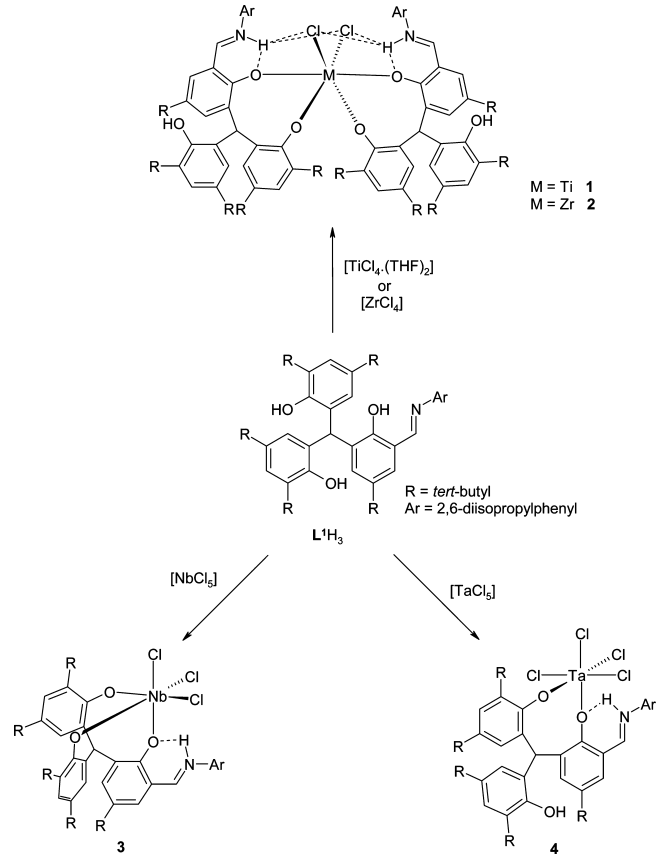

To date, much of the coordination chemistry of this imine tripod ligand family is restricted to complexes of aluminum and of nickel,[22,26] while in a preliminary communication, we have reported the complex $[VO(\mathbf{L^1}H_2)_2]$ (L^1H_2 is the monodeprotonated form of 3-[2,2′-methylenebis(4,6-di-*tert*-butylphenol)-5-*tert*-butylsalicylidene-(2,6-diisopropyl)phenylimine]), (Scheme 1) which upon activation with dimethylaluminum chloride (DMAC) was found to be active for ethylene homopolymerization.[27] We have now embarked upon a synthetic program to study the coordinating characteristics of this relatively new class of phenoxyimine ligand family. Here, we present our results using the early transition metals, specifically of groups IV and V, and report results of their polymerization behavior toward ethylene in the presence of a variety of organoaluminum cocatalysts.

Results and Discussion

The condensation reaction to form the pendant imine arm of $\mathbf{L^1}H_3$[28] was carried out in refluxing ethanol for 1 h with a catalytic amount of formic acid. Upon cooling of the reaction mixture, removal of solvent in vacuo yielded $\mathbf{L^1}H_3$ as a crude yellow solid. Extraction into hot acetonitrile, followed by slow evaporation, produced yellow/green prisms suitable for single crystal X-ray analysis (Figure 2).

(22) Scott, M. J.; Cottone, A.; Morales, D.; Lecuivre, J. L. *Organometallics* **2002**, *21*, 418.
(23) (a) Matsui, S.; Tohi, Y.; Mitani, M.; Saito, J.; Makio, H.; Tanaka, H.; Matsukawa, N.; Nitabaru, M.; Nakano, T.; Kashiwa, N.; Fujita, T. *Chem. Lett.* **1999**, 1065. (b) Fujita, T.; Saito, J.; Mitani, M.; Mohri, J.; Yoshida, Y.; Matsui, S.; Ishii, S.; Kojoh, S.; Kashiwa, N. *Angew. Chem. Int. Ed.* **2001**, *40*, 2918. (c) Matsui, S.; Mitani, M.; Saito, J.; Tohi, Y.; Makio, H.; Matsukawa, N.; Takagi, Y.; Tsuru, K.; Nitabaru, M.; Nakano, T.; Tanaka, H.; Kashiwa, N.; Fujita, T. *J. Am. Chem. Soc.* **2001**, *123*, 6847. (d) Matsui, S.; Fujita, T. *Catal. Today* **2001**, *66*, 63. (e) Mitani, M.; Mohri, J.; Yoshida, Y.; Saito, J.; Ishii, S.; Tsuru, K.; Matsui, S.; Furuyama, R.; Nakano, T.; Tanaka, H.; Kojoh, S.; Matsugi, T.; Kashiwa, N.; Fujita, T. *J. Am. Chem. Soc.* **2002**, *124*, 3327. (f) Mitani, M.; Furuyama, R.; Mohri, J.; Saito, J.; Ishii, S.; Terao, H.; Kashiwa, N.; Fujita, T. *J. Am. Chem. Soc.* **2002**, *124*, 7888. (g) Makio, H.; Kashiwa, N.; Fujita, T. *Adv. Synth. Catal.* **2002**, *344*, 477. (h) Furuyama, R.; Saito, J.; Ishii, S.; Mitani, M.; Matsui, S.; Tohi, Y.; Makio, H.; Matsukawa, N.; Tanaka, H.; Fujita, T. *J. Mol. Catal.* **2003**, *200*, 31. (i) Nakayama, Y.; Bando, H.; Sonobe, Y.; Suzuki, Y.; Fujita, T. *Chem. Lett.* **2003**, *32*, 766. (j) Nakayama, Y.; Bando, H.; Sonobe, Y.; Fujita, T. *Bull. Chem. Soc. Jpn.* **2004**, *77*, 617. (k) Nakayama, Y.; Bando, H.; Sonobe, Y.; Fujita, T. *J. Mol. Catal.* **2004**, *213*, 141. (l) Makio, H.; Fujita, T. *Bull. Chem. Soc. Jpn.* **2005**, *78*, 52. (m) Fujita, T.; Furuyama, R.; Saito, J.; Ishii, S.; Makio, H.; Mitani, M.; Tanaka, H. *J. Organomet. Chem.* **2005**, *690*, 4398.
(24) Fujita, T.; Tohi, Y. (Mitsui. Chemicals. Inc.) Eur. Patent 874,005,A1, 1998.
(25) Bryliakov, K. P.; Kravtsov, E. A.; Pennington, D. A.; Lancaster, S. J.; Bochmann, M.; Brintzinger, H. H.; Talsi, E. P. *Organometallics* **2005**, *24*, 5660.
(26) Libra, E. R.; Scott, M. J. *Chem. Commun.* **2006**, 1485.
(27) Redshaw, C.; Rowan, M. A.; Homden, D. M.; Dale, S. H.; Elsegood, M. R. J.; Matsui, S.; Matsuura, S. *Chem. Commun.* **2006**, 3329.
(28) Synthesis of the previously reported proligand $\mathbf{L^1}H_3$ (see Figure 2 and Scheme 1) was carried out following the method of Scott et al. with benzylamine replaced by 2,6-diisopropylaniline (see ref 22).

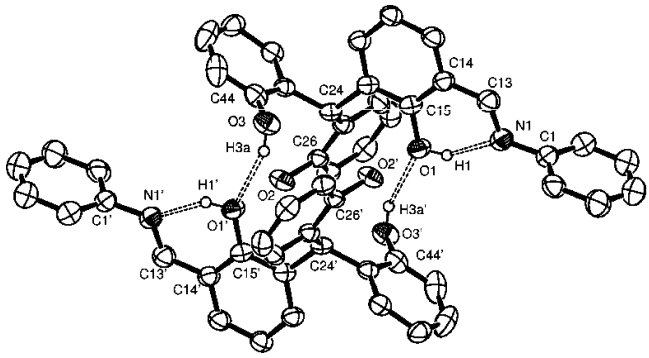

Figure 2. ORTEP representation of the structure of $\mathbf{L^1}H_3$. Hydrogen atoms (except H1 and H3a) have been omitted for clarity; thermal ellipsoids are drawn at the 50% probability level.

Both intramolecular and intermolecular hydrogen bonding is observed in $\mathbf{L^1}H_3$. The intramolecular interaction involves the nitrogen atom of the imine arm and the closest phenolic group: O(1)−H(1)···N(1) [O···N = 2.604(4) Å]. The intermolecular hydrogen bonds O(3)–H(3A)···O(1′) [O···O = 2.971(6) Å] are formed by the same oxygen atom, acting as an acceptor, and a free phenolic unit from a second ligand molecule. The two molecules form a pseudo-16-membered ring system about a center of inversion.

Titanium and Zirconium. The reaction between $[TiCl_4(THF)_2]$ or $[ZrCl_4]$ and $\mathbf{L^1}H_3$ at a 1:1 ratio in refluxing toluene, followed by removal of solvents in vacuo and extraction into warm acetonitrile, afforded the complexes **1** and **2** as deep red diamonds and yellow blocks (yields of 83% and 81%), respectively.

Single crystal X-ray analysis of both species show similar complexes of the form $[MCl_2(\mathbf{L^1}H_2)_2]$ (M = Ti (**1**); Zr (**2**)), both exhibiting a metal oxidation state of +4. In **1**, there is a crystallographic 2-fold symmetry axis through the titanium atom; in **2** the two metal-bound ligands are only pseudo-symmetrical (there are also two independent molecules in the asymmetric unit). Both **1** and **2** show iminium species by X-ray analysis (three crystals of each were selected at random), with C═N bond lengths of 1.290(3) Å for **1** and in the range of 1.286(4)−1.299(3) Å for **2**. In each instance, the hydrogen atom attached to the nitrogen was located in the Fourier difference map.

Complexes **1** and **2** are both bis-chelating, with each metal center displaying a pseudo-octahedral environment with four oxygens (from two ligands) and two *cis*-chlorine atoms bound to the metal center completing the coordination sphere; angles around the metal centers range from 82° to 100°.

With titanium (Figure 3, Table 1a), the Ti−O bond lengths are within the normal range for these types of bonds.[23c,29,30] As expected, Ti−O(1) is elongated [1.9744(14) Å compared to Ti−O(2), 1.8509(13) Å] because of a reduction in π-donation ability caused by additional hydrogen bonding to the iminium hydrogen: N(5)−H(5)···O(1) [N···O = 2.714(2) Å]. There is also additional hydrogen bonding between an unbound phenolic unit of one chelating ligand and its symmetry related equivalent in the second chelated ligand: O(36)−H(36)···O(36′) [O···O = 2.876(2) Å]. The Ti−Cl bond length [2.4789(6) Å] is longer than that observed in similar phenoxyimine systems [2.261(2)−2.305(2) Å],[23b,m] again the likely cause being the additional hydrogen bonds to the iminium proton: N(5)−H(5)···Cl(1′) [N···Cl = 3.301(3) Å].

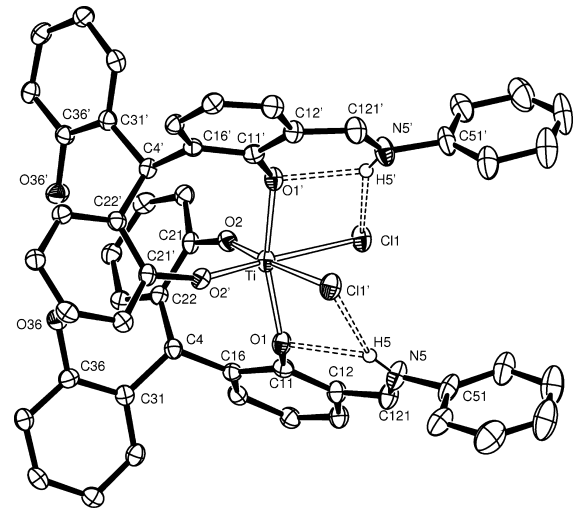

Figure 3. ORTEP representation of the structure of **1**. Alkyl groups, solvent molecules of acetonitrile, and hydrogen atoms (except H5 and H5′) have been omitted for clarity; thermal ellipsoids are drawn at the 50% probability level.

Table 1. Selected Bond Lengths (Å) and Angles (deg) with Estimated Standard Deviations of **1** and **2**

(a)		(b)	
Ti−O(1)	1.9744(14)	Zr(1)−O(11)	2.1078(18)
Ti−O(2)	1.8509(13)	Zr(1)−O(71)	1.9804(18)
Ti−Cl(1)	2.4789(6)	Zr(1)−Cl(11)	2.5529(7)
O(1)−Ti−O(1′)	164.17(8)	O(11)−Zr(1)−O(61)	167.57(7)
O(1)−Ti−O(2)	95.33(6)	O(11)−Zr(1)−O(21)	93.70(7)
O(1)−Ti−O(2′)	94.92(6)	O(11)−Zr(1)−O(71)	94.35(7)
O(1)−Ti−Cl(1)	85.39(4)	O(11)−Zr(1)−Cl(11)	85.94(5)
O(1)−Ti−Cl(1′)	82.79(4)	O(11)−Zr(1)−Cl(12)	84.25(5)
O(2)−Ti−Cl(1′)	171.98(5)	O(21)−Zr(1)−Cl(12)	172.11(6)

In the case of the zirconium compound **2** (Table 1b), a similar pattern is observed. The $Zr-O_{phenolate}$ bond lengths [av 1.977 Å] are within previously reported ranges,[23c,29,30] with longer $Zr-O_{imine}$ bonds [2.0886(19)−2.1078(18) Å] because of hydrogen bonding: N−H···O [N···O(av) = 2.709 Å]. The Zr−Cl bonds [2.5351(8)−2.5529(7) Å] are also longer than previously reported values for N−H···Cl hydrogen bonding[29,30] [N···Cl(av) = 3.3505 Å].

Niobium. The reaction between $\mathbf{L^1}H_3$ and $[NbCl_5]$ at a 1:1 ratio in refluxing toluene produced, after extraction into acetonitrile and prolonged standing at −25 °C, X-ray quality orange/red crystals of $[NbCl_3(\mathbf{L^1}H)]$ (**3**) (Scheme 1) in good yield (51%). The solid state structure of **3** (Figure 4) revealed a mononuclear zwitterionic structure, with two independent molecules, whose bond lengths and angles are essentially identical, in the asymmetric unit. The environment around the niobium(V) center is pseudo-octahedral formed by the three oxygens of the ligand molecule and three chlorine atoms arranged in a *fac*-manner. The presence of an iminium species was confirmed by the C−N bond lengths of 1.279(7) and 1.295(7) Å in the two molecules, with the hydrogen

(29) Bott, R. K. J.; Hughes, D. L.; Schormann, M.; Bochmann, M.; Lancaster, S. J. *J. Organomet. Chem.* **2003**, *665*, 135.
(30) Zhang, D.; Jin, G. X. *Appl. Catal. A* **2004**, *262*, 85.

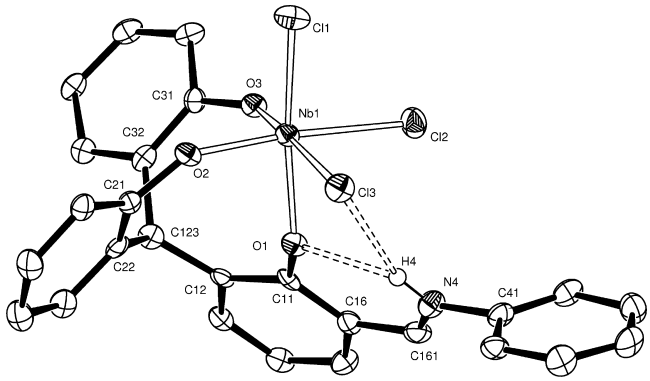

Figure 4. ORTEP representation of the structure of one of the independent molecules of **3**. Alkyl groups, three molecules of acetonitrile and hydrogen atoms (except H4) have been omitted for clarity; thermal ellipsoids are drawn at the 50% probability level.

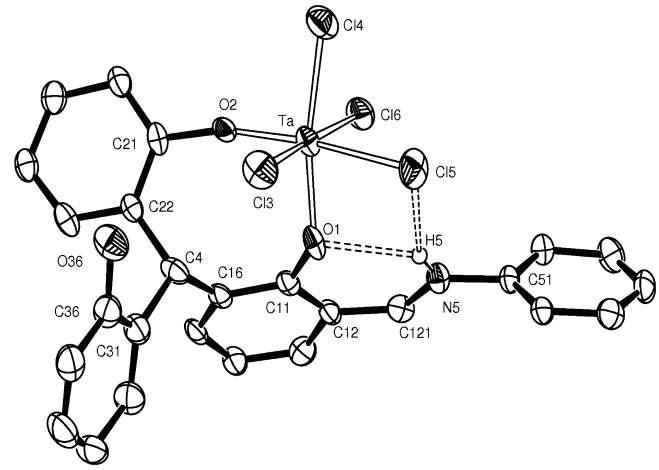

Figure 5. ORTEP representation of the structure of **4**. Alkyl groups and hydrogen atoms (except H5) have been omitted for clarity; thermal ellipsoids are drawn at the 50% probability level.

atoms attached to the nitrogen atoms being located in a Fourier difference map. Once again hydrogen bonding to the protonated phenol is observed, with an N···O average distance of 2.671 Å. ^{1}H NMR spectroscopy indicates retention of the solid state structure in solution, displaying a doublet for the N=C*H* proton at 7.92 ppm because of coupling to the iminium hydrogen. The coupling constant (^3J = 15.9 Hz) is close to that reported by Scott et al. (^3J = 14.4 Hz), for the related complex [$(L^2)^+$AlMe$^-$].[22]

The Nb···$O_{phenolate}$ distances [av 1.872 Å] lie within the range previously observed for niobium aryloxide bonds [1.730(5)−1.985(4) Å].[11] The niobium−oxygen bond formed by the phenolate group located next to the iminium species (Nb−O_{imine}), displays a significantly longer bond length [av 2.003 Å], a possible explanation being the reduction in π-donation from the oxygen atom because of its involvement in hydrogen bonding (vide supra). Two Nb−Cl bonds [av 2.387 Å] lie within previously reported Nb−Cl values [2.250(6)−2.4339(10) Å];[11] the third Nb−Cl_{imine} bond is longer [av 2.456 Å], possibly because of the additional hydrogen bond to the iminium species: N···Cl(av) = 3.43 Å.

Tantalum. Analogous reaction conditions using a 1:1 ratio of [$TaCl_5$] and $\mathbf{L^1}H_3$ led to the isolation of bright yellow crystals in high yield (62%) (Scheme 1). An X-ray diffraction study revealed a monomeric complex of the form [$TaCl_4$($\mathbf{L^1}H_2$)] (**4**), whose structure is shown in Figure 5 with bond lengths and angles given in Table 2.

The structure of **4** is similar to that of the niobium analogue; here, however, four chlorines are bound to the metal center, the extra chlorine taking preference over the binding of a second phenolate group. The geometry around the metal center is again octahedral, with two *cis*-oxygen atoms and four chlorine atoms completing the coordination sphere.

The presence of an iminium species was confirmed by a C(121)−N(5) bond length of 1.280(6) Å with the hydrogen atom attached to N(5) located in a Fourier difference map. The two Ta−O bonds lie within the range for previously

Table 2. Selected Bond Lengths (Å) and Angles (deg) with Estimated Standard Deviations of **4**

Ta−O(1)	1.965(4)
Ta−O(2)	1.845(4)
Ta−Cl(3)	2.3771(18)
Ta−Cl(4)	2.3329(18)
Ta−Cl(5)	2.4078(15)
Ta−Cl(6)	2.3639(16)
O(1)−Ta−O(2)	93.85(15)
O(1)−Ta−Cl(3)	92.93(11)
O(1)−Ta−Cl(4)	169.09(12)
O(1)−Ta−Cl(5)	81.38(11)
O(1)−Ta−Cl(6)	86.79(11)
Cl(3)−Ta−Cl(6)	177.38(6)
O(2)−Ta−Cl(5)	173.99(13)

reported bond lengths [1.8375(18)−2.025(7) Å][31] but differ considerably in length from one another. Similar reasoning to that of the niobium analogue can be applied here: the oxygen atom of the longer Ta−O(1) bond is also involved in hydrogen bonding to the iminium group, N(5)···O(1) = 2.791 Å, leading to a reduction in π-donation to the metal center, evident also by the reduction in carbon−oxygen−metal bond angle [C(11)−O(1)−Ta = 134.9(3)° compared with C(21)−O(2)−Ta = 163.7(4)°]. The Ta−Cl bonds are all very similar and lie within previously reported values [1.913(2)−2.500(1) Å];[31] the longest bond length is Ta−Cl(5), in which the chlorine atom is also involved in hydrogen bonding: N(5)−H(5)···Cl(5) [N···Cl = 3.334 Å].

Vanadium-imido Chemistry. In the following section, we have chosen to use alkoxide starting materials rather than vanadium oxytrichloride for two reasons: namely, we have found that liberated HCl can be problematic, particularly when using imido compounds, and second, our previous experience using the oxytrisalkoxides, [$VO(OR)_3$], has revealed a pronounced tendency for forming highly crystalline materials. The reaction between $\mathbf{L^1}H_3$ (3-[2,2′-methylenebis(4,6-di-*tert*-butylphenol)-5-*tert*-butylsalicylidene-(2,6-diisopropyl)phenylimine]) and [V(N*p*-tol)(O*n*-Pr)$_3$] produced the acetonitrile-insoluble complex [{V(N-*p*-tol)($\mathbf{L^1}H_1$)}$_2$(μ-

(31) (a) Mulford, D. R.; Clark, J. R.; Schweiger, S. W.; Fanwick, P. E.; Rothwell, I. P. *Organometallics* **1999**, *18*, 4448. (b) Thorn, M. G.; Parker, J. R.; Fanwick, P. E.; Rothwell, I. P. *Organometallics* **2003**, *22*, 4658.

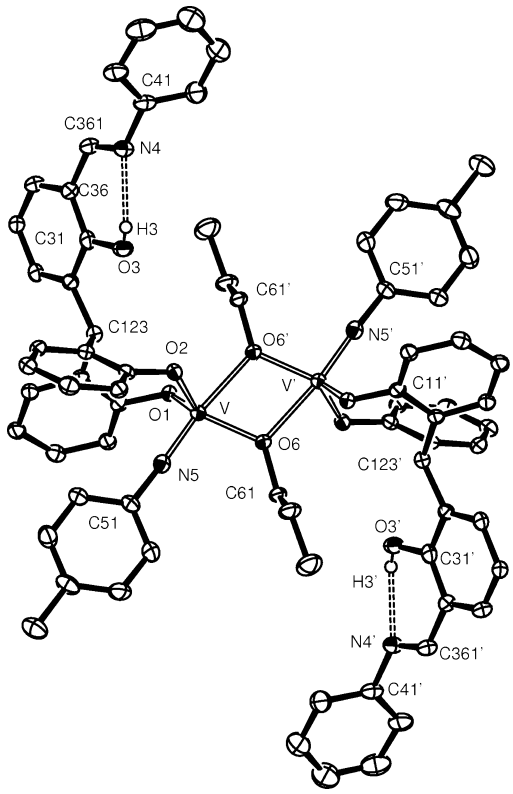

Figure 6. ORTEP representation of the structure of **5**. Alkyl groups (except C541 and C541′) and hydrogen atoms (except H3 and H3′) have been omitted for clarity; thermal ellipsoids are drawn at the 50% probability level.

Table 3. Selected Bond Lengths (Å) and Angles (deg) with Estimated Standard Deviations of **5**

V−O(1)	1.826(2)
V−O(2)	1.824(2)
V−N(5)	1.664(3)
V−O(6)	1.866(2)
V−O(6′)	2.178(2)
O(2)−V−O(1)	109.47(10)
N(5)−V−O(1)	98.90(12)
O(1)−V−O(6)	118.07(10)
O(1)−V−O(6′)	86.31(9)
N(5)−V−O(2)	97.88(12)
O(2)−V−O(6)	124.55(10)
O(2)−V−O(6′)	84.78(9)
N(5)−V−O(6)	101.19(12)
N(5)−V−O(6′)	172.91(12)
O(6)−V−O(6′)	72.01(10)

O*n*-Pr)$_2$] (**5**) (**L**^{1}H$_1$ = doubly deprotonated **L**^{1}H$_3$) in good yield (70%). Crystals suitable for X-ray diffraction were grown from a saturated solution of dichloromethane on prolonged standing (2−3 days) at ambient temperature. Structural analysis revealed a dimeric arrangement, formed though two asymmetrically bridged *n*-propoxide groups (Figure 6, Table 3); the asymmetric nature is apparent in the differing bond lengths, V−O(6) 1.866(2) Å, being within the range for a formal bonding interaction, compared to the longer V−O(6′) 2.178(2) Å, which is indicative of a dative interaction. A center of symmetry is located between the bridging alkoxide groups.

The environment around the vanadium center is best described as pseudo trigonal bipyramidal with one metal center bonding to two phenolate oxygens and an alkoxide oxygen in the equatorial sites; an almost linear imido group [C(51)−N(5)−V = 174.4(2)°] and a datively bound alkoxide occupy the axial positions. Unlike that previously found in the vanadyl case,[27] here the phenoxy-imine group does not interact with the metal center, rather it is involved in intramolecular hydrogen bonding: O(3)−H(3)···N(4) [O···N = 2.633(4) Å]. The V−O phenoxide bonds [1.826(2) and 1.824(2) Å] and V=N imido bond [1.664(3) Å] are normal with respect to previously reported structures of V(V) aryloxide complexes [V−O in the range of 1.754(5)−1.8632(13) Å; V=N in the range of 1.652(2)–1.669(3) Å].[12,32]

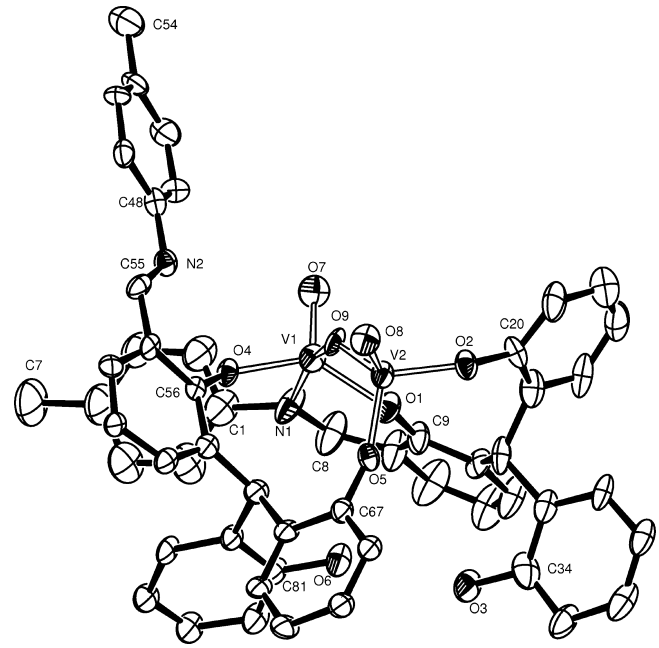

Figure 7. ORTEP representation of one of the two independent molecules of **6**. Alkyl groups (except C7 and C54), solvent molecules of acetonitrile, and hydrogen atoms have been omitted for clarity; thermal ellipsoids are drawn at the 30% probability level.

A second complex, [(VO)$_2$(μ-O)(**L**^{3}H)$_2$] (**6**) (**L**^{3}H = doubly deprotonated (3-[2,2′-methylenebis(4,6-di-*tert*-butylphenol)-5-*tert*-butylsalicylidene-*p*-tolylimine]) was isolated from the acetonitrile fraction of the filtration as brown needles in low yield (25%). Structural analysis using synchrotron radiation,[33] revealed a bimetallic system (Figure 7) with a bridging oxo group and the chelation of two ligand molecules also bridging the metal centers each through two of the three phenolic oxygens. Two independent molecules are found in the asymmetric unit and possess similar geometrical parameters. There is no retention of the imido group from the metal precursor, the loss presumably caused by hydrolysis accounting for the two vanadyl functionalities observed. Surprisingly, an imido exchange has occurred between the initial vanadium-bound imido group and the pendant imine arm such that the 2,6-diisopropylphenyl groups have been replaced by the *p*-tolyl groups. In the solid-state structure, V(2) is found to be tetrahedral in geometry, the other V(1)

(32) Redshaw, C.; Gibson, V. C.; Elsegood, M. R. J. *J. Chem. Soc., Dalton Trans.* **2001**, 767.

(33) (a) Clegg, W.; Elsegood, M. R. J.; Teat, S. J.; Redshaw, C.; Gibson, V. C. *J. Chem. Soc., Dalton Trans.* **1998**, 767. (b) Clegg, W. *J. Chem. Soc., Dalton Trans.* **2000**, 3223.

approximately square pyramidal with the vanadyl group in the apical position and the vanadium atom positioned 0.52 Å out of the square-based plane; the increased coordination of V(2) is caused by the binding of one of the pendant imine arms. Both vanadyl bond lengths are typical; however the $V-O_{phenoxide}$ bond lengths about V_{sp} in comparison to V_{tet} vary dramatically. In the case of V_{tet}, the increase in Lewis acidity of the metal center (caused by the lower coordination number) shortens the V−O bond lengths [1.696(7)−1.808(6) Å]. On the other hand, V_{sp} displays longer bonds [1.880(8)−1.972(8) Å] more akin to those seen in **I** and **7**, where the additional donation by the imine nitrogen leads to a decrease in the Lewis acidity of the metal center. Because of this difference in the Lewis acidity of the two vanadium centers, the bridging oxygen is asymmetric [av $V_{sp}-O$ 1.9675 = Å; $V_{tet}-O$ = 1.709 Å] and acts as O^{2-} giving each metal center a +5 oxidation state.

In solution, complex **6** adopts a different geometry. The ^{1}H NMR spectrum shows only one set of sharp peaks for the hydrogen atoms, implying that in solution the complex is C_2-symmetric. The ^{1}H NMR spectrum also displays a single sharp resonance at ∼4.20 ppm that integrates to 2 hydrogens; although the phenolic hydrogens could not be located in the difference map, the NMR data implies that these hydrogens, with such a downfield shift, are involved in a dramatic level of hydrogen bonding within the complex. Both metal centers are V(V) and give two distinct peaks in the ^{51}V NMR at $\delta = -510.4$ and -567.2 ppm. The mass spectrum shows a single peak at 1525.9, showing clearly the molecular ion peak and also the relative stability of the complex.

Bis-Capped System. Given the bidentate chelating nature of the ligands observed in complexes **1**−**5**, we targeted a ligand system with sufficient binding sites to satisfy the coordination needs of a vanadium center. To this end, the precursor 3-[2,2′-methylenebis(4,6-di-*tert*-butylphenol)-5-*tert*-butyl-2-hydroxybenzaldehyde ($\mathbf{L^0}H_3$) was reacted with *o*-phenylenediamine (1,2-diaminobenzene) in a 2:1 molar ratio. Reaction in refluxing ethanol with a catalytic amount of formic acid for 1 h, removal of solvent, and recrystallization from hot acetonitrile gave $\mathbf{L^5}H_6$ in moderate yield (50%). Structural analysis (Figure 8) shows a pseudo 16-membered macrocyclic structure because of a series of intramolecular hydrogen bonds (Table 4) involving both phenolic and imine groups (cf., $\mathbf{L^1}H_3$).

Both H(31) and H(71) were located on the Fourier difference map, indicating the presence of both an imine and iminium species within the ligand backbone. As in **1**, **2**, and **4**, the ^{1}H NMR spectrum of $\mathbf{L^5}H_6$ shows that in solution the imine species predominates, exhibiting singlets at δ 8.65 and 8.19 ppm (each 1H) for each of the imine groups; the presence of two peaks resulting from the differing nature of hydrogen bonding related with each imine moiety. A single peak in the mass spectrum at *m*/*z* 1273 represents the moleular ion, while bands in the IR spectrum at 1622 and 1576 cm^{-1} are assignable to the two C=N stretches.

A change in the molar ratio of $\mathbf{L^0}H_3$ to *o*-phenylenediamine from 2:1 to 1:1 and an extended reaction time of 12 h produced a bright orange compound $\mathbf{L^6}H_3$ in low yield (18%). Crystals of $\mathbf{L^6}H_3$ were grown from a saturated ethanol solution, and X-ray diffraction revealed the formation of a benzimidazolyl moiety rather than the phenoxy-imine moieties previously seen (Figure 9).

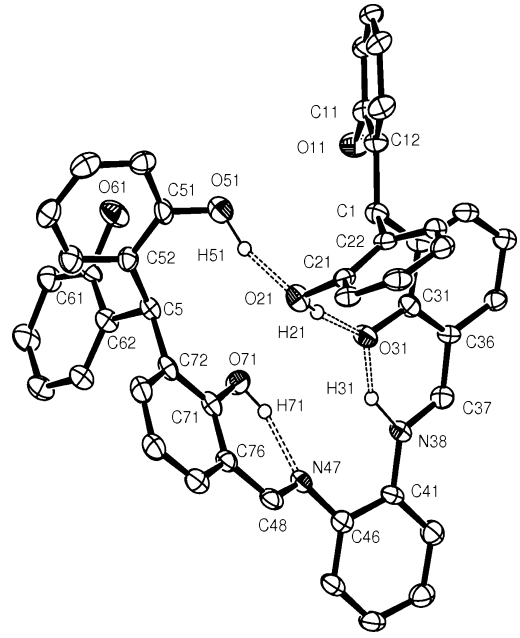

Figure 8. ORTEP representation of the structure of $\mathbf{L^5}H_6$. Alkyl groups, solvent molecules of acetonitrile, and hydrogen atoms (except H21, H31, H51, and H71) have been omitted for clarity; thermal ellipsoids are drawn at the 50% probability level.

Table 4. Hydrogen Bond Parameters for $\mathbf{L^5}H_6$

	D−H (Å)	D−H···A (deg)	D···A (Å)	H···A (Å)
O(21)−H(21)···O(31)	0.98(4)	167(3)	2.713(3)	1.75(4)
N(38)−H(31)···O(31)	1.26(5)	143(3)	2.560(3)	1.44(5)
O(51)−H(51)···O(21)	1.06(5)	164(4)	2.708(3)	1.68(5)
O(71)−H(71)···N(47)	0.91(3)	151(3)	2.604(3)	1.77(3)

Proligand $\mathbf{L^6}H_3$ exhibits two intramolecular hydrogen bonds in the solid state: O(1)−H(1)···N(1) [donor−acceptor = 2.563(3) Å] and O(3)−H(3)···O(1) [donor−acceptor = 2.832(3) Å] (Figure 9). As a result, the mean planes of the imidazole ring [N(1)−C(9)] and the benzene ring bearing O(1) [C(2)−C(7)] have almost parallel normal vectors: the angle between these is 6.75°. The benzimidazole groups in

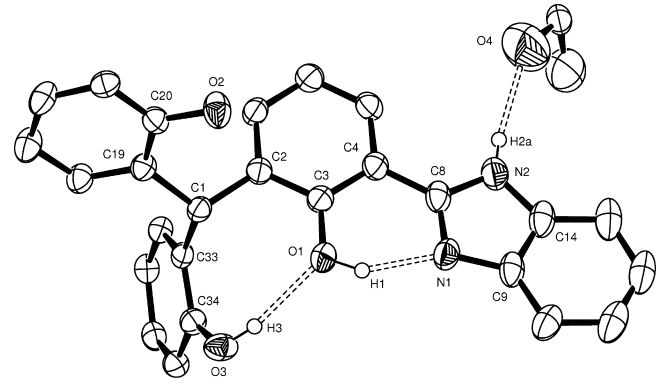

Figure 9. ORTEP representation of the structure of $\mathbf{L^6}H_3$. Alkyl groups, one molecule of ethanol, and hydrogen atoms (except H1, H2a, and H3) have been omitted for clarity; thermal ellipsoids are drawn at the 50% probability level.

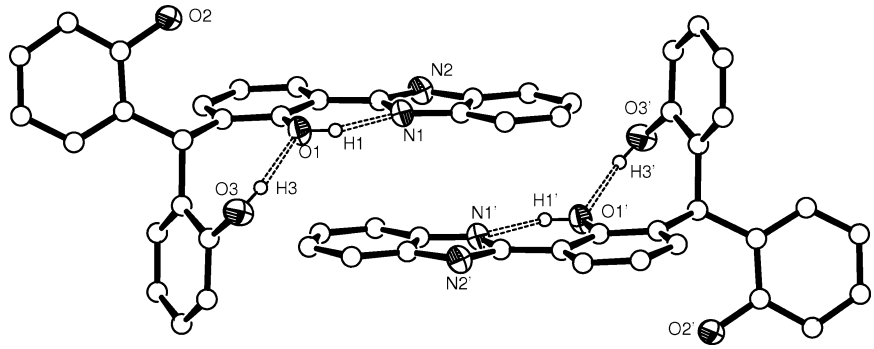

Figure 10. View of $\mathbf{L^6H_3}$ illustrating intramolecular hydrogen bonding and π-stacking of benzimidazoze group.

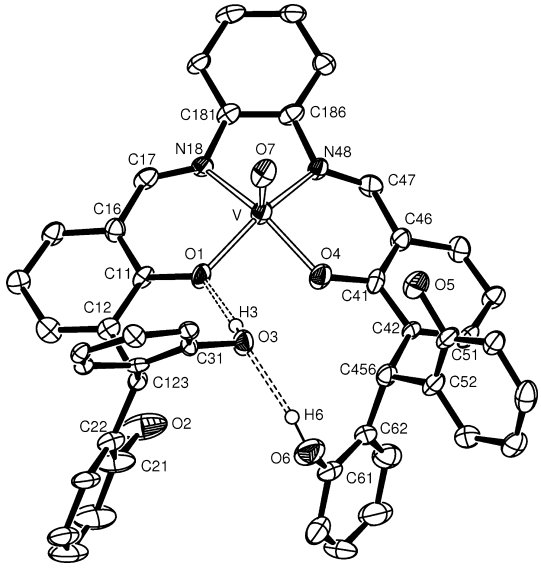

Figure 11. ORTEP representation of the structure of **7**. Minor component V2−O(7A), alkyl groups, solvent molecules of acetonitrile and hydrogen atoms (except H3 and H6) have been omitted for clarity; thermal ellipsoids are drawn at the 50% probability level.

Table 5. Selected Bond Lengths (Å) and Angles (deg) with Estimated Standard Deviations of **7**

V−O(7)	1.599(4)	V2−O(7A)	1.604(17)
V−O(1)	1.950(3)	V2−O(1)	1.956(10)
V−N(18)	2.055(4)	V2−N(18)	2.117(10)
V−N(48)	2.043(4)	V2−N(48)	2.155(10)
V−O(4)	1.937(3)	V2−O(4)	2.014(10)
V···V(2)	1.374(9)		
O(7)−V−O(1)	110.62(17)	O(7A)−V2−O(1)	110.0(7)
O(7)−V−O(4)	110.58(16)	O(7A)−V2−O(4)	115.4(6)
O(7)−V−N(18)	103.47(16)	O(7A)−V2−N(18)	109.6(7)
O(7)−V−N(48)	104.11(18)	O(7A)−V2−N(48)	114.0(7)
N(18)−V−O(4)	145.28(15)	N(18)−V2−O(4)	134.5(5)
N(48)−V−O(1)	144.71(16)	N(48)−V2−O(1)	135.6(5)

$\mathbf{L^6H_3}$ are arranged in antiparallel π-stacks (Figure 10). The planes defined by the 5-membered imidazole rings are 3.422 Å apart, with a centroid−centroid distance of 3.485 Å.

The reaction of $\mathbf{L^5H_6}$ with [VO(O-*n*-Pr)$_3$] in refluxing toluene afforded, after workup into acetonitrile, black prisms of the complex [(VO)($\mathbf{L^5H_4}$)] (**7**) in moderate yield (33%). During the reaction the metal center is reduced from V(V) to V(IV).

Structural analysis (Figure 11, Table 5) indicates the presence of two forms of the complex with the vanadyl group pointing above or below the N_2O_2 plane [deviation of 0.594 Å for major component, 0.897(3) site occupancy; 0.778 Å for minor component, 0.103(3) site occupancy]; however, only the principal component is shown. Occupying the cavities opposite the vanadyl centers are disordered molecules of acetonitrile. In each case, the vanadium center is five coordinate and can be best described as having a square pyramidal geometry. The binding of the metal center is through both phenoxy-imine groups of the ligand in an analogous manner to the previously reported nickel and palladium structures by Scott et al.,[26] such that the remaining four phenols remain unaffected.

The result of using *o*-phenylenediamine to form a bridged bis-imine ligand is that binding of the metal center to the phenoxy-imine moieties can only proceed in a cis manner compared to that of **I,** wherein the two free phenoxy-imine arms bind trans with respect to each other. Although the difference between the cis and trans binding motifs does not appear to affect bond lengths dramatically, the rigidity of the central phenyl ring in the *o*-phenylenediimine group produces a more symmetrical binding of the metal center with trans angles in the N_2O_2 plane in **7** deviating by less than 1°. In the case of **I**, the lack of conformational rigidity is evident by trans angles in the N_2O_2 plane deviating by over 23°. Of the remaining unbound phenolic groups in **7**, two form hydrogen bonds within the ligand: O(3)−H(3)···O(1) [donor−acceptor = 2.784(5) Å] and O(6)−H(6)···O(3) [donor−acceptor = 2.852(6) Å]; the latter bonds intramolecularly to an opposite arm of the ligand forming a pseudo-macrocycle similar to that seen with the parent pro-ligand (Figure 8). The remaining two phenolic hydrogens have no close neighbors.

The use of $\mathbf{L^5H_6}$ in a 2:1 molar ratio with [VO(O*n*-Pr)$_3$], under analogous conditions to those used for **7**, produced small dark brown needles of [(VO)$_2$($\mathbf{L^5H}$)] (**8**) in moderate yield (33%). Structural characterization by single-crystal X-ray crystallography (Figure 12, Table 6) revealed the binding of two vanadium centers; the binding of the vanadyl groups proceeds in an identical manner to that of **7** with the V(IV) center, V(1), adopting a square-based pyramidal geometry, with the vanadium located 0.628 Å out of the mean plane of the basal atoms [O(1), O(4), N(18), and N(48)]. A second vanadyl group, V(2)−O(8), is bound through three of the remaining phenolic units in a tetrahedral arrangement.

The bond lengths about V(1) are similar to those found in **7**; however the binding of a second vanadium atom drasti-

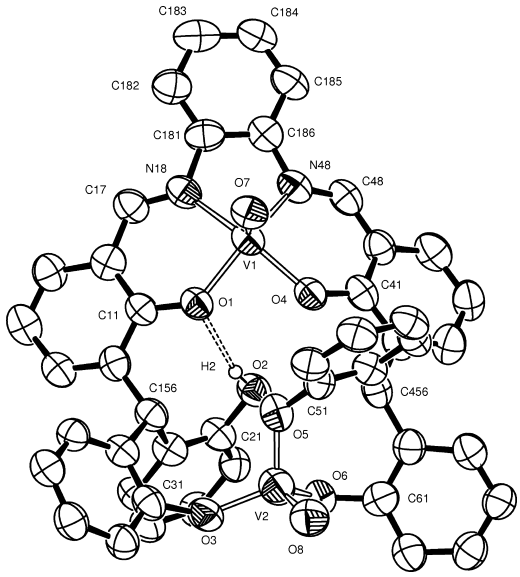

Figure 12. ORTEP representation of the structure of **8**. Alkyl groups, hydrogen atoms (except H2), and solvent molecules of acetonitrile have been omitted for clarity; thermal ellipsoids are drawn at the 50% probability level.

Table 6. Selected Bond Lengths (Å) and Angles (deg) with Estimated Standard Deviations of **8**

V(1)−N(18)	2.056(6)
V(1)−N(48)	2.059(6)
V(1)−O(1)	1.914(5)
V(1)−O(4)	1.926(5)
V(1)−O(7)	1.594(5)
V(2)−O(3)	1.784(5)
V(2)−O(5)	1.764(5)
V(2)−O(6)	1.777(5)
V(2)−O(8)	1.589(6)
O(1)−V(1)−O(4)	86.39(19)
O(1)−V(1)−N(18)	86.4(2)
O(1)−V(1)−N(48)	137.3(2)
O(1)−V(1)−O(7)	113.0(2)
O(4)−V(1)−N(18)	148.1(2)
O(3)−V(2)−O(5)	113.1(2)
O(3)−V(2)−O(6)	110.1(2)
O(3)−V(2)−O(8)	112.6(3)
O(5)−V(2)−O(8)	105.3(3)
O(5)−V(2)−O(6)	109.3(2)
O(6)−V(2)−O(8)	106.2(3)

cally alters the angles around V(1). Comparisons show that for **8** the angles around V(1) are closer to those of the trans-bound complex **I** with trans angles varying by 11°. Because of the flexibility and rotational freedom of the phenolic groups, the angles around V(2) are close to ideal for tetrahedral geometry, deviating by a maximum of 4°. The V−O and V═O bond lengths around V(2) are all within previously stated ranges (vide supra). The one remaining free hydroxyl group hydrogen bonds intramolecularly to O(1): O(2)−H(2)···O(1) [donor−acceptor = 2.780(6) Å]. The ^{1}H NMR spectrum of **8** shows broad, featureless lines because of the paramagnetic V(IV) center within the complex, while a peak at *m*/*z* 1402 in the mass spectrum shows the $[M - O]^+$ peak; the composition has also been confirmed by CHN analysis.

Ligand $\mathbf{L^6}H_3$ (Figures 9 and 10) was reacted with [V(O)(O*n*-Pr)$_3$] at a 2:1 ratio affording, following workup, the analogous (to that of **I**) bis-chelating structure $[VO(\mathbf{L^6}H_2)_2]$ **9** in 61% yield. The purity of the complex was confirmed by microanalysis; Evans' method NMR experiment, together with EPR measurements, verified the presence of a V(IV) species.

Changing Aniline. Proligands 3-[2,2′-methylenebis(4,6-di-*tert*-butylphenol)-5-*tert*-butylsalicylidene-R-imine, where R = NC_6H_5 ($\mathbf{L^2}H_3$), NC_6H_4Me ($\mathbf{L^3}H_3$) and $NC_6H_2Me_3$ ($\mathbf{L^4}H_3$) were synthesized using a 1:1 ratio of the appropriate aniline to $\mathbf{L^0}H_3$ in refluxing ethanol with a catalytic amount of formic acid. Upon removal of solvents in vacuo, ^{1}H NMR spectroscopy indicated that the crude products were pure and needed no further recrystallization. Following the method previously published by our group,[27] the vanadyl bearing complexes $[VO(\mathbf{L^{2-4}}H_2)_2]$ (**10**−**12**) were synthesized in low yields (20−26%) of high purity as indicated by elemental analysis. In all cases, a reduction occurred at the metal center from V(V) to V(IV), as confirmed by magnetic moment measurements by Evans' method[34] and EPR.

Oxidation States of Vanadium Complexes. During the extensive reactions involving different vanadium alkoxide starting materials both V(V) and V(IV) species have been isolated and characterized in the final complexes. The V(V) species were characterized by ^{1}H and ^{51}V NMR, shifts for which are given in Table 7.[12] For V(IV) systems, the magnetic moment and EPR isotropic and anisotropic values are given in Table 8.

The ^{51}V NMR shifts for **5** and **6** follow trends that have previously been noted. The shift for **5** is typical of the range previously observed for the O_4N donor set, while for **6** the peaks at δ −510.43 and −567.23 are consistent with VO_3N and VO_4 environments, respectively.[35] In particular it has been found that imido-bearing vanadium centers display peaks shifted to more positive values compared to those arising from vanadyl groups. The corresponding line widths for imido groups are also broader than those of oxo groups. A plot of the inverse line-width against chemical shift for **5** and **6** revealed two distinct environments for the vanadium atoms.[36] Results suggest that in solution complex **5** exhibits a 4-coordinate vanadium center arising, most probably, from cleavage of both dative alkoxide bonds leading to a monomeric complex. In solution, complex **6** displays two 5-coordinate vanadium centers, which can be achieved by interactions of the two metal centers with the two imine nitrogen atoms.

All V(IV) species were characterized by room-temperature and low-temperature (40 K) X-band EPR measurements. As expected, a characteristic 8-line spectrum (d^1) was obtained in all cases at room temperature (I = 7/2). Anisotropic parameters were collected from frozen toluene solutions, analysis of which (as well as room temperature results) were carried out by simulation using SIMFONIA.[37] Values for $g_\perp$ and $g_\parallel$ (Table 8) compare well with those reported previously for oxovanadium(IV) systems,[38a,b] and in-

(34) Evans, D. F. *J. Chem. Soc.* **1959**, 2003.
(35) (a) Santoni, G.; Licini, G.; Rehder, D. *Chem. Eur. J.* **2003**, *9*, 4700. (b) Rehder, D.; Weidemann, C.; Duch, A.; Priebsch, W. *Inorg. Chem.* **1988**, *27*, 584. (c) Priebsch, W.; Rehder, D. *Inorg. Chem.* **1985**, *24*, 3058.
(36) Crans, D. C.; Shin, P. K. *J. Am. Chem. Soc.* **1994**, *116*, 1305.
(37) Simfonia, Bruker Analytische Messentechnik, GmbH, version 1.25, Shareware version, 1996.

Table 7. ^{51}V NMR Data for V(V) Complexes

complex	Δ (ppm)	$\omega_{1/2}$ (Hz)	ref
5	−480.84	320	this work
6	−510.43	60	this work
6	−567.23	80	this work
[V(O)-*tert*-butylhexahomooxacalix[3]arene]	−321.3	143	12
[V(N-*p*-tol)-*tert*-butylhexahomooxacalix[3]arene]	−216.2	1998	12
[{VO(O-*t*-Bu)}$_2$(μ-O)Cax(OMe)$_2$(O)$_2$]·2MeCN	−586.6	134	12
[{VO(O-*n*-Pr)}$_2$(μ-O)Cax(OMe)$_2$(O)$_2$]·2MeCN	−545.6	144	12
[VO(O-*t*-Bu)]$_2$(μ-O)Li$_4$O$_2$Cax(OMe)$_2$(O)$_2$]·8MeCN	−592.9	865	12
[V(N-*p*-tolyl)(O-*t*-Bu)$_2$Cax(OMe)$_2$(O)(OH)]·5MeCN	−352.8	353	12
[VOCax(O)$_3$(OMe)(NCMe)]	−354.6	907	12
[V(N-*p*-tolyl)Cax(O)$_3$(OMe)(NCMe)]	−332.6	925	12
[{VOCax(O)$_4$}$_2$(μ-2,6-(CH$_2$)$_2$C$_5$H$_5$N)]	−371.5	2170	12

Table 8. Magnetic Moments, Isotropic, and Anisotropic Values for V(IV) Complexes

complex	μ_{eff}	g_{iso}	A_{iso}	$g_\perp$	$A_\perp$	$g_{\|\|}$	$A_{\|\|}$
[VO(**L**^{1}H$_2$)$_2$] (**I**)[26]	1.76	1.99	94	1.98	67	1.95	185
[VO(**L**^{2}H$_2$)$_2$] (**10**)	1.33	2.01	96	1.99	64	1.95	185
[VO(**L**^{3}H$_2$)$_2$] (**11**)	1.33	1.98	96	1.99	65	1.95	185
[VO(**L**^{4}H$_2$)$_2$] (**12**)	1.39	2.01	95.5	1.99	64.5	1.96	180
[VO(**L**^{5}H$_4$)] (**7**)	1.15	1.99	95	1.99	65	1.96	183
[(VO)$_2$(**L**^{5}H)] (**8**)	1.83	1.99	100	1.99	64	1.96	181
[VO(**L**^{6}H$_2$)$_2$] (**9**)	1.86	2.00	95	1.99	63	1.96	186

particular with those reported for the VO[N_2O_2] coordination set, though the $A_{||}$ values are a little on the high side (usual range 160−170 × 10^{-4} cm^{-1}).[38c] Both isotropic and anisotropic parameters were found to be comparable in all cases implying similar metal environments for all complexes. Magnetic moments expected for oxovanadium(IV) complexes, when the orbital contribution is quenched, are 1.73 μ_B; experimentally observed values for complexes **7** and **10**−**12** were notably lower.

Insight into the Imine Functionality. The imine group in these complexes appears to be relatively inert. Attempts to reduce the C═N linkage using standard reducing agents such as $LiAlH_4$ and $NaBH_4$ were unsuccessful. Even 10-fold loadings of reducing agent led to the recovery of unreacted imine ligand. Furthermore, imines are known to react with trialkylaluminum reagents, with transfer of an alkyl group to the imine backbone often observed.[39] Here, however, treatment of **L**^{1}H$_3$ with trimethylaluminum (3.3 equivalents) afforded the complex {($AlMe_2$)[AlMe(NCMe)]**L**^{1}} (**13**) in moderate yield (38%). Single crystal X-ray analysis (Figure 13) shows **13** to be comparable to that previously reported by Scott et al.,[22] whose structure included a molecule of DMSO in place of the molecule of MeCN found in **13**. The complex displays two different Al(III) centers, one bound through the phenoxy-imine moiety with two methyl groups still intact, the second being bound to two phenolate oxygens with one methyl group on the aluminum center; the coordination sphere is completed by a molecule of solvent. Bond lengths and angles are given in Table 9 and compared to those of the structure previously reported by Scott.

All bond lengths and angles for **13** are comparable to those of the DMSO analogue (see Table 9) with both aluminum centers adopting pseudo tetrahedral geometry. It was found that upon increasing the molar ratio of proligand to aluminum to as high as 1:6, there was no evidence of methyl transfer to the imine backbone.

Ethylene Polymerization. Initial screening of complexes **1**−**4** (Scheme 1), employing a variety of organoaluminum cocatalysts [dimethylaluminum chloride (DMAC), methylaluminoxane (MAO), and trimethylaluminum (TMA)] at ambient temperature over prolonged time periods yielded negligible or no polymeric material, and further screening involving these complexes was not carried out.

Vanadium-based systems are emerging as a promising class of α-olefin polymerization catalyst.[12,23i,27,40] It was therefore not unexpected that procatalysts **5**−**12** and the previously reported procatalyst **I**, when screened in the presence of DMAC and the reactivating substance ethyl-

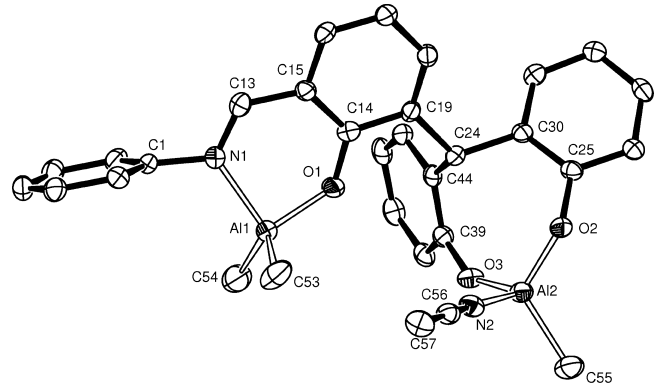

Figure 13. ORTEP representation of the structure of **13**. Alkyl groups, hydrogen atoms, and solvent molecules of acetonitrile have been omitted for clarity; thermal ellipsoids are drawn at the 50% probability level.

(38) (a) Selbin, J. *Chem. Rev.* **1965**, *65*, 153. (b) Costa Pessoa, J.; Calhorda, M. J.; Cavaco, I.; Correia, I.; Duarte, M. T.; Felix, V. *J. Chem. Soc., Dalton Trans.* **2002**, 4407. (c) Yue, H.; Zhang, D.; Shi, Z.; Feng, S. *Solid State Sci.* **2006**, *8*, 1368.

(39) (a) Gibson, V. C.; Redshaw, C.; White, A. J. P.; Williams, D. J. *J. Organomet. Chem.* **1998**, *550*, 453. (b) Bruce, M.; Gibson, V. C.; Redshaw, C.; Solan, G. A.; White, A. J. P.; Williams, D. J. *Chem. Commun.* **1998**, 2523. (c) Milione, S.; Cavallo, C.; Tedesco, C.; Grassi, A. *J. Chem. Soc., Dalton Trans.* **2002**, *8*, 1839. (d) Knijnenburg, Q.; Smits, J. M. M.; Budzelaar, P. H. M. *Organometallics* **2006**, *25*, 1036.

Table 9. Selected Bond Lengths (Å) and Angles (deg) with Estimated Standard Deviations of **13**

13		Scott complex[22]	
Al(1)−O(1)	1.7664(19)	Al(2)−O(3)	1.7726(15)
Al(1)−N(1)	1.979(2)	Al(2)−N(1)	1.980(2)
Al(1)−C(53)	1.946(3)	Al(2)−C(40)	1.943(3)
Al(1)−C(54)	1.946(3)	Al(2)−C(41)	1.961(3)
Al(2)−O(2)	1.731(2)	Al(1)−O(1)	1.7169(16)
Al(2)−O(3)	1.7018(19)	Al(1)−O(2)	1.7553(15)
Al(2)−C(55)	1.947(3)	Al(1)−C(39)	1.949(2)
Al(2)−N(2) (MeCN)	1.984(3)	Al(1)−O(4) (DMSO)	1.8238(16)
O(1)−Al(1)−N(1)	94.06(9)	O(3)−Al(2)−N(1)	93.66(8)
O(1)−Al(1)−C(53)	111.82(13)	O(3)−Al(2)−C(40)	110.39(10)
O(1)−Al(1)−C(54)	112.16(13)	O(3)−Al(2)−C(41)	110.37(10)
O(2)−Al(2)−O(3)	113.99(9)	O(1)−Al(1)−O(2)	115.11(7)
O(2)−Al(2)−C(55)	117.22(12)	O(1)−Al(1)−C(39)	111.10(10)
O(2)−Al(2)−N(2)	97.49(10)	O(1)−Al(1)−O(4)	107.31(7)

trichloroacetate (ETA), produced highly active polymerization systems (1000−7000 g/mmol h bar) as defined by the Gibson criteria.[1a]

The use of ETA as a reactivator in vanadium systems is now well established.[41] Extended reaction time profiles for the vanadium-based procatalysts displayed general trends previously observed for vanadium-based ethylene polymerization: an initial higher level of activity over the initial 5−10 min of the polymerization reaction, after which a decrease in activity (often as much as 50% of the initial value) leads to a lower but sustained level of polymerization.[12,27,40]

Procatalyst **5** produced the highest activity (∼6800 g/mmol h bar), higher than the isoelectronic vanadyl analogues; this again is a trend that has been previously observed.[12] Procatalysts **6** and **8** are the most active of the vanadyl-bearing complexes (activities of ∼5200 and 4200 g/mmol h bar, respectively), possibly because of a cooperative effect brought about by the close proximity of the two metal centers. Interestingly, for **7** (run 3) containing only one vanadyl center (cf., **8**), the activity is ∼2450 g/mmol h bar.

The previously reported procatalyst **I** exhibited a high level of initial activity (∼8500 g/mmol h bar) after 5 min; this system however is deactivated rapidly, producing a final sustained activity of 4200 g/mmol h bar. Similar activities (∼5900 g/mmol h bar) for **I** were observed previously under increasing diluted conditions; the slight increase in activity is caused by the reduction of mass transport issues.[27] The effect of substitution upon the pendent imine (Table 10, runs 6−9) produced activities in the range of ∼1000−4000 g/mmol h bar, with the trend, whereby the increased sterics of the aniline led to increased activity. The exact nature of the active species in these systems still remains unknown, although in the context of propylene polymerization Zambelli and Allegra have suggested that a 5-coordinate V(III) center is required to carry out the polymerization reaction,[42] with chlorines bridging the aluminum and vanadium centers, while Gambarotta et al. have postulated a vanadium−aluminum−phenoxide cluster that also contains chloro groups bridging the vanadium and aluminum centers.[40b] As mentioned earlier, for group IV phenoxyimine systems using *i*-Bu_3Al /$[CPh_3]$-$[B(C_6F_5)_4]$ as cocatalyst, phenoxyamine ligands have been isolated via hydrolysis of the catalyst solution.[23c,l] Such behavior, the result of the susceptibility of the imine group to attack by electrophiles, is not observed when using MAO as cocatalyst[23c] but cannot be overlooked in the present systems using DMAC.

Table 10. Polymerization Runs for **5**−**12** and **I** in the Presence of DMAC[a]

run	procatalyst	activity (g[PE]/ mmol[V] h bar)	M_w (g mol^{-1})	M_n (g mol^{-1})	PDI
1[b]	**5**	6798	236 000	98 200	2.4
2[c]	**6**	5204	262 000	107 000	2.5
3[c]	**7**	2452	245 000	102 000	2.4
4	**8**	4224	293 000	136 000	2.2
5[c]	**9**	3032	230 000	101 000	2.3
6	**10**	1062	226 000	81 100	2.8
7	**11**	1668	338 000	145 000	2.7
8	**12**	1948	137 000	46 300	2.8
9[c]	**I**	4192	110 000	37 900	2.9

[a] Conditions: 0.5 μmol of [V] per run, 50 mL of toluene, 45 °C, 5000 equiv DMAC, 0.1 mL of ETA, 60 min (unless otherwise indicated). GPC analysis was conducted in 1,2,4-trichlorobenzene against a polystyrene calibrant. [b] 20 min. [c] 30 min.

In this work (Table 10), all polymers obtained were of high molecular weight (monomodal), with narrow polydispersity indices (PDI), indicative of single-site catalysis. The melting points of the polymers fall within approximately a 2 °C range (133.9−136.1 °C) and are typical of linear polyethylene.

Full catalytic screening was carried out with the diisopropyl derivative **I**. The combination of the organoaluminum cocatalysts MAO/TMA, with and without the reactivator ETA, produced negligible or no polymer, whereas the use of DMAC without reactivator (Table 11, run 20) produced an active system, albeit with a level of activity an order of magnitude less than the corresponding run with reactivator present. Over the temperature range of 0−80 °C (Table 11, runs 10−14), the catalyst performed well, showing a good level of thermal stability with activities increasing with increasing temperature. However, for lifetime studies, a reaction temperature of 45 °C was chosen to prevent any mass transport issues often encountered at higher tempera-

(40) (a) Milione, S.; Cavallo, G.; Tedesco, C.; Grassi, A. *J. Chem. Soc., Dalton Trans.* **2002**, 1839. (b) Gambarotta, S. *Coord. Chem. Rev.* **2003**, *237*, 229. (c) Redshaw, C.; Warford, L.; Elsegood, M. R. J.; Dale, S. H. *Chem. Commun.* **2004**, 1954. (d) Tomov, A. K.; Gibson, V. C.; Zaher, D.; Elsegood, M. R. J.; Dale, S. H. *Chem. Commun.* **2004**, 1956. (e) Wang, W.; Nomura, K. *Macromolecules* **2005**, *38*, 5905.

(41) For early examples, see: (a) Gumboldt, A.; Helberg, J.; Schleitzer, G. *Makromol. Chem.* **1967**, *101*, 229. (b) Christman, D. L. *J. Polym. Sci., Part A* **1972**, *10*, 471. (c) Addison, E.; Deffieux, A.; Fontanille, M.; Bujadoux, K. *J. Polym. Sci., Part A: Polym. Chem.* **1994**, *32*, 1033.

(42) Zambelli, A.; Allegra, G. *Macromolecules* **1980**, *13*, 42.

Table 11. Variation of Temperature and DMAC Concentration during Ethylene Polymerization Using **I**[a]

run	temp (°C)	[Al]/[V]	activity (g[PE]/mmol h bar)	M_w (g mol^{-1})	M_n (g mol^{-1})	PDI
10	0	8000	2051	524 000	177 000	3.0
11	25	8000	4708	514 000	106 000	4.8
12	45	8000	7385	335 000	98 500	3.4
13	60	8000	17 324	200 000	53 100	3.8
14	80	8000	24 900	59 400	26 900	2.2
15	25	2000	0			
16	25	4000	2077	586 000	242 000	2.4
17	25	8000	3728	572 000	246 000	2.3
18	25	12 000	4327	621 000	159 000	3.9
19	25	16 000	7096	516 000	51 800	10.0
20[b]	45	5000	536	200 000	69 000	2.9

[a] Conditions: 0.5 mmol of [V] per run, 50 mL of toluene, 0.1 mL of ETA, 30 min. [b] Without ETA.

tures. As expected, increasing polymerization temperature led to a fall in molecular weight of the resulting polymer because of an increase in frequency of termination reactions compared to propagation reactions. The PDI of the polymers was found to increase slightly but was still suggestive of single site catalysis. With only 2000 equiv of DMAC (Table 11, run 15), no polymerization took place, presumably because of the need for a minimum quantity of cocatalyst to act as a scavenger. At 16 000 equiv of DMAC (Table 11, run 19), although the catalytic activity is increasing, the PDI of the resulting polymer was also found to have increased from a PDI of ~4 for 12 000 equiv of DMAC to a value of 10, suggesting that at such high [Al]/[V] ratios as 16 000:1, other reactions are occurring with multiple bond breakage leading to loss of single-site catalysis.

Conclusion

We have prepared and structurally characterized a number of group IV and V complexes containing imine-tripodal ligands. In the case of group IV metals (Ti and Zr), bischelating zwitterionic structures were observed and found to be inactive toward ethylene polymerization using a wide range of organoaluminum cocatalysts. Although in both cases *cis*-chlorines were present, it is thought that the steric bulk of the C-capped triphenol moiety shielded the metal center such that no polymer chain growth could occur. In the case of niobium and tantalum, monochelating zwitterionic structures were observed, which upon activation with common organoaluminum cocatalysts gave negligible activities.

The previously reported complex **I** was found to be highly active for the polymerization of ethylene using DMAC as cocatalyst in the presence of the reactivating agent ETA. Encouraged by these results, a family of vanadium-based imine-tripodal complexes were synthesized and screened as potential procatalysts. Complex **5**/DMAC/ETA, the vanadium−imido-bearing procatalyst, displayed the highest activities (~6800 g/mmol h bar), while for the vanadyl complexes, systems employing **6** and **8**, both of which contain two vanadyl groups, gave the highest activities ~5200 and 4200 g/mmol h bar, respectively. Where the pendent imine arm was formed from a substituted aniline, it was found that reduction in steric bulk of the substituted groups led to a reduction in activity, such that the diisopropyl derivative yielded the highest activities, while the unsubstituted aniline derivative **10** gave the lowest overall activity of ~1000 g/mmol h bar. All catalysts producing high molecular weight polymer with a narrow PDI for [Al]/[V] ratios of ≤12 000. Further screening of **I** gave evidence of a high degree of thermal stability (up to 80 °C) of these types of catalysts, although an increase in temperature led to a reduction in the molecular weight of the polymer (524 000 g mol^{-1} at 0 °C compared to 60 000 g mol^{-1} at 80 °C).

Experimental Section

General experimental and ethylene polymerization procedures were performed as described elsewhere.[12] The precursors 3-[2,2′-methylenebis(4,6-di-*tert*-butylphenol)-5-methyl-2-hydroxybenzaldehyde] $\mathbf{L^0H_3}$,[22] [$TiCl_4(THF)_2$],[43] and procatalyst **I**[27] were prepared as previously described. All other chemicals were obtained commercially and used as received unless otherwise stated.

Preparation of Ligands. Preparation of $\mathbf{L^2H_3}$. Aniline (0.17 mL, 1.83 mmol) and $\mathbf{L^0H_3}$ (1.00 g, 1.66 mmol) in ethanol (25 mL) were brought to reflux. A drop of formic acid was added to catalyze the reaction, and a Dean−Stark condenser was attached. The solution was refluxed for 1 h and then allowed to cool. The solvents were removed in vacuo affording $\mathbf{L^2H_3}$ as a yellow/orange powder. Yield: 660 mg, 59%. mp: 180 °C. $C_{46}H_{61}NO_3$ Calcd (found): C, 81.8 (81.7); H, 9.1 (9.1); N, 2.1 (2.1). ^{1}H NMR ($CDCl_3$, 400 MHz): δ 8.65 (1H, s, C*H*═N), 7.6−6.6 (11H, m, Ar−*H*), 6.10 (1H, s, Ar_3CH), 1.37 (18H, s, *t*-Bu), 1.17 (9H, s, *t*-Bu), 1.16 (18H, s, *t*-Bu). MS *m*/*z* (EI): 676 $(M)^+$. IR (Nujol mull, cm^{-1}): 3499m, 3452m, 3184w, 1619m, 1580m, 1293w, 1246w, 1188m, 1145w, 1118w, 1071w, 1021w, 974w, 943w, 924w, 877m, 819w, 753m, 718m, 664m.

Preparation of $\mathbf{L^3H_3}$. Preparation was done as for $\mathbf{L^2H_3}$ but using $\mathbf{L^0H_3}$ (1.00 g, 1.66 mmol) and *p*-toluidene (0.20 g, 1.83 mmol), affording $\mathbf{L^3H_3}$ as a yellow powder. Yield: 1.10 g, 96%. mp: 182 °C. $C_{47}H_{63}NO_3$ Calcd (found): C, 79.95 (79.95); H, 9.45 (9.50); N, 1.90 (1.81). ^{1}H NMR ($CDCl_3$, 400 MHz): δ 8.32 (1H, s, C*H*═N), 7.4−6.8 (10H, m, Ar−*H*), 6.08 (1H, s, Ar_3CH), 5.51 (2H, s, O*H*), 2.28 (3H, s, tolyl−CH_3), 1.37 (18H, s, $C(CH_3)_3$), 1.20 (9H, s, $C(CH_3)_3$), 1.18 (18H, s, $C(CH_3)_3$). MS *m*/*z* (EI): 690 $(M)^+$. IR (Nujol mull, cm^{-1}): 3188m, 2725m, 2656w, 1363m, 1287w, 1259m, 1187m, 1169w, 1151w, 1093m, 1014m, 982w, 874w, 860w, 838w, 802m, 716m.

Preparation of $\mathbf{L^4H_3}$. Preparation was done as for $\mathbf{L^2H_3}$ but using $\mathbf{L^0H_3}$ (1.00 g, 1.66 mmol) and 2,4,6-trimethylaniline (0.26 mL, 1.83 mmol) affording $\mathbf{L^4H_3}$as a bright yellow powder. Yield: 1.08 g, 82%. mp: 186 °C. $C_{49}H_{67}NO_3$ Calcd (found): C, 82.0 (81.9); H, 9.4 (9.5); N, 2.0 (2.1). ^{1}H NMR ($CDCl_3$, 400 MHz): δ 8.66 (1H, s, C*H*═N), 7.4−6.8 (10H, m, Ar−*H*), 6.10 (1H, s, Ar_3CH), 5.40 (2H, s, O*H*),

(43) Manzer, L. E. *Inorg. Synth.* **1982**, *21*, 84.

Table 12. Crystallographic Data

compound	**1**	**2**	**3**	**4**	**5**
formula	$C_{104}H_{144}Cl_2N_2O_6Ti$, $2(C_2H_3N)$	$C_{104}H_{144}Cl_2N_2O_6Zr$, $\sim 4(C_2H_3N)$, $0.25(C_7H_8)$	$C_{52}H_{71}Cl_3NNbO_3$, $\sim 3(C_2H_3N)$	$C_{52}H_{72}Cl_4NO_3Ta$, $3.5(C_2H_3N)$	$C_{124}H_{170}N_4O_8V_2$, $2(CH_2Cl_2)$
fw	1719.1	1867.6	1080.5	1225.5	2116.4
cryst syst	monoclinic	triclinic	monoclinic	monoclinic	triclinic
space group	*C*2/*c*	$P\bar{1}$	$P2_1/c$	*I*2/a (equiv to No. 15)	$P\bar{1}$
unit cell dimensions					
a (Å)	22.5593(14)	17.6990(8)	25.9531(12)	23.034(2)	12.0913(4)
b (Å)	18.0058(10)	23.4574(10)	17.4694(9)	17.0436(11)	15.5389(5)
c (Å)	27.3838(4)	27.3144(12)	28.2274(16)	30.5814(11)	17.3764(6)
α (deg)	90	79.896(4)	90	90	79.498(3)
β (deg)	113.416(5)	81.388(4)	103.711(4)	95.200(14)	85.991(3)
γ (deg)	90	79.655(4)	90	90	67.110(3)
V (Å^3)	10207.2(9)	10900.7(8)	12433.2(11)	11956.5(15)	2957.30(17)
Z	4	4	8	8	1
temp (K)	140(1)	140(1)	140(1)	140(1)	140(1)
radiation, *λ* (Å)	0.71073	0.71073	0.71073	0.71073	0.71073
D_{calcd} (g cm^{-3})	1.119	1.138	1.154	1.362	1.188
abs coeff (mm^{-1})	0.189	0.203	0.364	2.063	0.305
cryst size (mm)	0.40 × 0.35 × 0.25	0.55 × 0.40 × 0.28	0.57 × 0.44 × 0.22	0.34 × 0.09 × 0.06	0.38 × 0.31 × 0.17
$2\theta_{max}$ (deg)	45.2	50.0	50.0	45.0	48.0
reflns measured	43681	119030	122400	50712	27662
unique reflns, R_{int}	6697, 0.045	38169, 0.065	21787, 0.120	7791, 0.100	9214, 0.091
reflns with $F^2 > 2\sigma(F^2)$	5067	23808	13995	5269	5928
transm factors	0.995−1.004	0.997−1.003	0.981−1.024	none	0.978−1.028
params	573	2338	1242	654	661
R_1 [$F^2 > 2\sigma(F^2)$]	0.037	0.053	0.078	0.038	0.061
R_2 (all data)	0.101	0.127	0.200	0.075	0.153
largest difference peak and hole (e Å^{-3})	0.25 and −0.34	0.56 and −0.51	1.60 and −0.97	0.92 and −0.55	0.46 and −0.65

compound	**6**	**7**	**8**	**13**	**L^{5}H$_6$**	**L^{6}H$_3$**
formula	$C_{94}H_{122}N_2O_9V_2$	$C_{86}H_{114}N_2O_7V$, $\sim 2(C_2H_3N)$	$C_{97.3}H_{127.95}N_{7.65}O_8V_2$	$C_{59.13}H_{85.38}Al_2N_{3.06}O_3$	$C_{86}H_{116}N_2O_6$, $1.5(C_2H_3N)$	$C_{50}H_{72}N_2O_5$
fw	1525.82	1420.8	1634.40	941.01	1335.4	781.10
cryst syst	triclinic	monoclinic	triclinic	monoclinic	triclinic	monoclinic
space group	$P\bar{1}$	$P2_1/c$	$P\bar{1}$	$P2_1/n$	$P\bar{1}$	$P2_1/n$
unit cell dimensions						
a (Å)	13.458(10)	13.5859(6)	15.975(5)	13.0501(3)	11.3116(4)	9.5893(7)
b (Å)	26.862(19)	16.9639(8)	16.346(5)	18.1745(4)	17.2622(7)	25.8662(18)
c (Å)	27.87(2)	37.5567(18)	18.858(5)	24.7238(6)	23.1474(7)	19.0454(13)
α (deg)	99.998(8)	90	82.468(5)	90	108.022(3)	90
β (deg)	97.768(7)	97.957(4)	80.972(5)	95.7714(14)	90.477(3)	100.216(2)
γ (deg)	98.934(7)	90	78.492(5)	90	107.745(3)	90
V (Å^3)	9666(12)	8572.4(7)	4740(2)	5834.2(2)	4067.2(3)	4649.1(6)
Z	4	4	2	4	2	4
temp (K)	150(2)	140(1)	120(2)	120(2)	140(1)	150(2)
radiation, *λ* (Å)	0.7848	0.71073	0.71073	0.71073	0.71073	0.71073
D_{calcd} (g cm^{-3})	1.049	1.101	1.145	1.071	1.090	1.116
abs coeff (mm^{-1})	0.244	0.169	0.254	0.092	0.067	0.071
cryst size (mm)	0.40 × 0.10 × 0.06	0.67 × 0.25 × 0.14	0.20 × 0.15 × 0.04	0.22 × 0.08 × 0.06	0.7 × 0.20 × 0.12	0.91 × 0.28 × 0.12
$2\theta_{max}$ (deg)	50	40	45	50	45.0	52.86
reflns measured	52248	54018	53762	48327	31856	41353
unique reflns, R_{int}	25091, 0.1303	7931, 0.135	12208, 0.0919	10299, 0.0794	10483, 0.078	9541, 0.0569

Table 12. Continued

compound	6	7	8	13	L^5H_6	L^6H_3
reflns with $F^2 > 2\sigma(F^2)$	10 404	5049		7020	5391	5861
transm factors	0.909−0.986	0.988−1.017	0.582−0.990	0.980−0.995	0.964−1.031	0.939−0.992
params	2165	962	1092	629	924	581
R_1 [$F^2 > 2\sigma(F^2)$]	0.1436	0.064	0.1149	0.0623	0.051	0.0901
R_2 (all data)	0.3799	0.125	0.3570	0.1544	0.119	0.2998
largest difference peak and hole (e Å^{-3})	0.535 and −0.492	0.32 and −0.17	0.665 and −0.693	0.309 and −0.348	0.38 and −0.31	1.059 and −0.644

2.38 (3H, s, tolyl-*p*-C*H*$_3$), 2.16 (6H, s, tolyl-*o*-C*H*$_3$), 1.37 (18H, s, *t*-Bu), 1.20 (9H, s, *t*-Bu), 1.17 (18H, s, *t*-Bu). MS *m*/*z* (EI): 718 $(M)^+$. IR (Nujol mull, cm^{-1}): 3506m, 3487m, 3417bm, 3172bm, 1623m, 1592m, 1359m, 1285w, 1246w, 1192w, 1153w, 1118w, 1009w, 978w, 928w, 877w, 811w, 765w, 714w, 660m.

Preparation of L^5H_6. L^0H_3 (1.00 g, 4.27 mmol) and *o*-phenylenediamine (0.23 g, 2.14 mmol) were brought to reflux in ethanol (25 mL). A catalytic amount of formic acid was added and the reflux maintained for 1 h. The solvent was removed under reduced pressure, and the solid was recrystallized from hot acetonitrile (30 mL) to give L^5H_6 as orange prisms. Yield: 1.35 g, 50%. mp: 149−154 °C. $C_{86}H_{116}N_2O_6$ Calcd (found): C, 81.09 (81.19); H, 9.18 (9.26); N, 2.20 (2.19). ^{1}H NMR ($CDCl_3$, 400 MHz): δ 8.63 (2H, s, C*H*═N), 7.31−6.79 (16H, overlapping signals, Ar−*H*), 6.77 (4H, s, O*H*), 6.18 (2H, s, Ar_3CH), 1.26 (27H, s, *t*-Bu), 1.17 (27H, s, *t*-Bu), 1.14 (36H, s, *t*-Bu). MS *m*/*z* (MALDI): 1273 $(M)^+$. IR (Nujol mull, cm^{-1}): 3508bm (N−H stretch), 3339bm, 3176bm, 2364w, 1782w, 1709w, 1686w, 1622m (C═N stretch), 1576m, 1528w, 1417m, 1363m, 1295m, 1261m, 1244m, 1213m, 1190s, 1151m, 1121m, 1026m, 971w, 931w, 882m, 817m, 802m, 769m, 745m, 722m, 668m, 647m.

Preparation of L^6H_3. L^0H_3 (1.00 g, 4.27 mmol) and *o*-phenylenediamine (0.46 g, 4.27 mmol) were brought to reflux in ethanol (100 mL). A catalytic amount of formic acid was added, and the reflux was maintained for 12 h. The solution was cooled and filtered to give L^6H_3 as an orange powder. Yield: 525 mg, 18%. mp: 264 °C. $C_{46}H_{62}N_2O_3$ Calcd (found): C, 80.20 (79.97); H, 9.07 (9.13); N, 4.07 (4.12). ^{1}H NMR ($CDCl_3$, 400 MHz): δ 8.67 (1H, s, O*H*), 7.36−7.19 (6H, overlaying signals, Ar−*H*), 7.16 (2H, s, Ar−*H*), 6.81 (2H, s, Ar−*H*), 6.19 (1H, s, Ar_3CH), 5.71 (2H, bs, O*H*), 1.26 (18H, s, *t*-Bu), 1.18 (9H, s, *t*-Bu), 1.15 (18H, s, *t*-Bu). MS *m*/*z* (MALDI): 690 $(M + H)^+$. IR (Nujol mull, cm^{-1}): 3293bs, 2726m, 2267m, 2248m, 1588m, 1460s, 1417m, 1378s, 1359s, 1300m, 1258m, 1211m, 1161m, 1118m, 1091m, 1060m, 1033m, 994m, 873m, 838m, 803m, 784m, 765w, 733w, 726w, 667w.

Preparation of Complexes. Preparation of $[TiCl_2(L^1H_2)_2]$ (1). $[TiCl_4(THF)_2]$ (0.27 g, 0.81 mmol) and L^1H_3 (0.60 g, 0.79 mmol) were combined in a Schlenk flask in a glovebox. Toluene (40 mL) was added, and the solution was refluxed for 12 h. Upon cooling, the solvents were removed in vacuo, and the residue was extracted into warm acetonitrile (30 mL) affording **1** as deep red prisms upon standing at ambient temperature (1−2 days). Yield: 0.56 g, 83%. mp: 237 °C (dec). $C_{104}H_{144}N_2O_6Cl_2Ti$ Calcd (found): C, 76.59 (76.30); H, 8.63 (8.87); N, 1.70 (1.71). ^{1}H NMR ($CDCl_3$, 400 MHz) δ: 7.67 (2H, s, C═N*H*), 7.59 (2H, d, ^3J 15.9 Hz, C*H*═N), 7.49−6.00 (18H, overlapping signals, Ar−*H*), 4.95 (2H, s, Ar_3CH), 3.63 (2H, bm, *i*-Pr), 3.11 (2H, bm, *i*-Pr), 1.20−0.98 (114H, overlapping signals, *t*-Bu and *i*-Pr). MS *m*/*z* (FAB): 1563 $(M - 2Cl)^+$, 759 $(ligand)^+$. IR (Nujol mull, cm^{-1}): 3478m (N−H stretch), 2959s, 2897m, 2866m, 2359m, 2330w, 1634s (C═N stretch), 1544m, 1463s, 1390w, 1362m, 1332w, 1265m, 1230s, 1168m, 1122m, 1024w, 904w, 881w, 858m, 797m, 761m, 737m, 666w.

Preparation of $[ZrCl_2(L^1H_2)_2]$ (2). Preparation was done as for **1** but using $[ZrCl_4]$ (0.14 g, 0.60 mmol) and L^1H_3 (0.40 g, 0.53 mmol) affording **2** as yellow prisms upon standing at ambient temperature (1−2 days). Yield: 0.40 g, 81%. mp: >250 °C. $C_{104}H_{144}N_2O_6Cl_2Zr$ Calcd (found): C, 74.57 (74.34); H, 8.69 (8.64); N, 1.74 (1.67). ^{1}H NMR ($CDCl_3$, 400 MHz): δ 7.98 (2H, s, C═N*H*), 7.89 (2H, d, ^3J 19.9 Hz, C*H*═N), 7.49−6.75 (18H, overlapping signals, Ar−*H*), 5.12 (2H, s, Ar_3CH), 3.68 (2H, bm, *i*-Pr), 3.28 (2H, bm, *i*-Pr), 1.39−1.22 (114H, overlapping signals,

t-Bu and *i*-Pr). MS *m*/*z* (FAB): 1679 (M − H)$^+$, 1642 (M − Cl − 2H)$^+$, 759 (ligand)$^+$. IR (Nujol mull, cm^{-1}): 3458m (N−H stretch), 1635m (*C*═N stretch), 1557w, 1544w, 1303m, 1280m, 1261m, 1230m, 1211m, 1168m, 1120w, 1022m, 972m, 853m, 816m, 766m, 736m.

Preparation of [NbCl$_3$(L^{1}H)] (3). Preparation was done as for **1** but using [NbCl$_5$] (0.39 g, 1.45 mmol) and **L^1**H$_3$ (1.00 g, 1.32 mmol). Prolonged standing (4−5 days) at −25 °C afforded orange/red plates of **3.** Yield: 0.31 g, 24%. Further crops of **3** can be obtained from the mother liquor upon concentration and consequent isolation. Total yield: 0.65 g, 51%. mp: 217 °C (dec). $C_{52}H_{71}NO_3Cl_3Nb$ Calcd (found): C, 65.24 (65.43); H, 7.47 (7.47); N, 1.46 (1.50). ^{1}H NMR ($CDCl_3$, 400 MHz): δ 7.92 (1H, d, ^3J = 15.9 Hz, C*H*═N), 7.60 (1H, s, *C*═N*H*), 7.37−7.06 (9H, overlapping signals, Ar−*H*), 5.17 (1H, s, Ar$_3$C*H*), 3.16 (2H, septet ^3J = 7.0 Hz, *i*-Pr), 1.43 (18H, s, *t*-Bu), 1.29 (27H, s, *t*-Bu), 1.18 (12H, s, *i*-Pr). MS *m*/*z* (FAB): 921 (M − Cl)$^+$, 886 (M − 2Cl)$^+$, 851 (M − 3Cl)$^+$, 759 (ligand)$^+$. IR (Nujol mull, cm^{-1}): 3584m (N−H stretch), 1631m (*C*═N stretch), 1593m, 1590m, 1407w, 1377s, 1365s, 1325w, 1261m, 1222m, 1202m, 1156m, 1135m, 1097m, 1059w. 1027m, 921m, 909w, 899m, 859s, 800s, 762m, 738w, 726w, 676w, 665m, 625m.

Preparation of [TaCl$_4$(L^{1}H$_2$)] (4). Preparation was done as for **1** but using [TaCl$_5$] (0.52 g, 1.45 mmol) and **L^1**H$_3$ (1.00 g, 1.32 mmol), affording **4** as pale yellow plates upon standing at ambient temperature (5−6 days). Yield: 0.89 g, 62% . mp: 219 °C (dec). $C_{52}H_{72}NO_3Cl_4Ta$ Calcd (found): C, 57.73 (57.87); H, 6.71 (6.70); N, 1.29 (1.50). ^{1}H NMR ($CDCl_3$, 400 MHz): δ 7.96 (1H, s, C*H*═N), 7.46−6.92 (9H, overlapping signals, Ar−*H*), 4.96 (1H, s, Ar$_3$C*H*), 3.35 (1H, bm, *i*-Pr), 3.13 (1H, bm, *i*-Pr), 1.56 (9H, s, *t*-Bu), 1.35 (9H, s, *t*-Bu), 1.33 (12H, s, *i*-Pr), 1.31 (9H, s, *t*-Bu), 1.26 (9H, s, *t*-Bu), 1.18 (9H, s, *t*-Bu). MS *m*/*z* (FAB): 1081 (M)$^+$, 1046 (M − Cl)$^+$, 1011 (M − 2Cl)$^+$, 975 (M − 3Cl)$^+$, 759 (ligand)$^+$. IR (Nujol mull, cm^{-1}): 3540bm, 2363w, 1638m (*C*═N stretch), 1597w, 1561w, 1459m, 1377m, 1366m, 1260m, 1217m, 1092s, 1019s, 863w, 799s, 666m.

Preparation of [(VN-*p*-tol(L^{1}H))$_2$(μ-O-*n*-Pr)$_2$] (5) and [(VO)$_2$(μ-O)(L^{3}H)$_2$] (6). [VN-*p*-tol(O-*n*-Pr)$_3$] (0.44 g, 1.32 mmol) and **L^1**H$_3$ (1.00 g, 1.32 mmol) were combined in a dry box. Toluene (30 mL) was added, and the solution refluxed for 12 h. Upon cooling, the solvents were removed in vacuo, and the residue was extracted into warm acetonitrile (30 mL).

Compound **5**was isolated as an orange/red solid upon filtration. Yield: 900 mg, 70%. mp: 157 °C (dec). $C_{124}H_{170}N_4O_8V_2$ Calcd (found): C, 76.52 (76.59); H, 8.80 (8.76); N, 2.88 (2.79). ^{1}H NMR (C_6D_6, 400 MHz): δ 8.22 (2H, s, C*H*═N), 7.95 (2H, s, Ar−*H*), 7.88 (4H, s, Ar−*H*), 7.70 (2H, bs, O*H*), 7.26 (4H, s, Ar−*H*), 7.26−6.97 (8H, overlapping signals, Ar−*H*), 7.10 (2H, s, Ar$_3$C*H*), 6.40 (4H, d, ^3J 8 Hz, N-*p*-tol), 6.10 (4H, d, ^{3}J 8 Hz, N-*p*-tol), 5.95 (4H, bm, O-*n*-Pr), 2.94 (4H, sept, ^3J = 6.8 Hz, *i*-Pr), 2.77 (4H, bm, O-*n*-Pr), 1.80 (6H, s, N-*p*-tol), 1.73 (24H, s, *i*-Pr), 1.37 (36H, s, *t*-Bu), 1.24 (18H, s, *t*-Bu), 1.05 (18H, s, *t*-Bu), 1.03 (18H, s, *t*-Bu), 0.94 (6H, t, ^3J = 7.2 Hz, O-*n*-Pr). ^{51}V (C_6D_6, 105.1 MHz): δ −480.84 ($\omega_{1/2}$ = 320). MS *m*/*z* (Maldi): 760 (ligand)$^+$. IR (Nujol mull, cm^{-1}): 3464m, 3165m, 2718m, 2656m, 1619m (*C*═N stretch),1584m, 1541m, 1258m, 1211w, 1207w, 1168w, 1100m, 1017w, 974w, 881m, 842m, 800m, 757m, 726m.

Compound **6** was isolated as dark brown crystals from the filtrate. Yield: 248 mg, 25%. mp: 85 °C (dec). $C_{94}H_{122}N_2O_9V_2$ Calcd (found): C, 74.0 (73.9); H, 8.1 (8.0); N, 1.8 (1.9). ^{1}H NMR (C_6D_6, 400 MHz): δ 7.55 (2H, s, C*H*═N), 7.48−7.39 (10H, overlapping signal, Ar−*H*), 7.15 (6H, overlapping signal, Ar−*H*) 6.83 (4H, d, ^3J = 8 Hz, N-*p*-tol), 6.71 (2H, s, Ar−*H*), 6.57 (4H, d, ^3J = 8 Hz, N-*p*-tol), 6.22 (2H, Ar$_3$C*H*), 4.19 (2H, s, O*H*), 1.97 (6H, s, N-*p*-tol), 1.75 (18H, s, *t*-Bu), 1.39 (18H, s, *t*-Bu), 1.35 (18H, s, *t*-Bu), 1.25 (18H, s, *t*-Bu), 1.21 (18H, s, *t*-Bu). ^{51}V (C_6D_6, 105.1 MHz): δ −510.43 ($\omega_{1/2}$ = 60), −567.23 ($\omega_{1/2}$ = 80). MS *m*/*z* (MALDI): 1526 (M)$^+$. IR (Nujol mull, cm^{-1}): 3495m, 1611m, 1603m, 1553w, 1502,m 1308m, 1269m, 1242m, 1184m, 1153m, 1122m, 1075m, 1040m, 1017m, 982s, 924m, 869m, 827m, 811m, 765w, 722m, 664m.

Preparation of [VO(L^{5}H$_4$)] (7). To a solution of **L^5**H$_6$ (1.00 g, 0.79 mmol) in toluene (30 mL) was added [VO(O-*n*-Pr)$_3$] (0.18 mL, 0.79 mmol). The solution was refluxed overnight before being cooled, and the solvent was removed in vacuo. The crude material was extracted into acetonitrile (40 mL) and filtered giving **7** as purple brown plates. Yield: 350 mg, 33%. mp: >250 °C. $C_{86}H_{114}O_7N_2V$ Calcd (found): C, 76.91 (77.15); H, 8.61 (8.58); N, 2.17 (2.09). MS *m*/*z* (Maldi): 1337.6 (M + H)$^+$. IR (Nujol mull, cm^{-1}): 3379m, 2725w, 2364w, 1607w, 1591m, 1546m, 1413w, 1364m, 1330m, 1311m, 1261s, 1197m, 1161m, 1099bs, 1018bs, 976m, 926m, 882m, 847m, 802s, 741m, 673m, 661m. Magnetic moment: μ = 1.15 μ_B. EPR (toluene, 298 K): g_{iso} = 1.99, A_{iso} = 95 G; (toluene, 10 K) $g_\perp$ = 1.99, $A_\perp$ = 65 G, $g_{||}$ = 1.96, $A_{||}$ = 183 G.

Preparation of [(VO)$_2$(L^{5}H)] (8). To a solution of **L^5**H$_6$ (1.00 g, 0.79 mmol) in toluene (30 mL) was added [VO(O-*n*-Pr)$_3$] (0.10 mL, 0.40 mmol). The solution was refluxed overnight before being cooled, and the solvent was removed in vacuo. The crude material was extracted into acetonitrile (40 mL) and filtered, giving **8** as a yellow/brown solid. Yield: 680 mg, 62%. mp: >350 °C. $C_{86}H_{111}O_8N_2V_2$ Calcd (found): C, 73.6 (73.6); H, 8.0 (8.0); N, 2.0 (2.1). MS *m*/*z* (MALDI): 1401 (M − O)$^+$. IR (Nujol mull, cm^{-1}): 3499m, 3335m, 1604m, 1580m, 1539m, 1460m, 1440m, 1376m, 1362m, 1330w, 1291w, 1215w, 1194m, 1154m, 1115m, 1099m, 1020m, 996m, 924w, 908w, 874m, 844m, 803m, 768m, 753m, 722w. Magnetic moment: μ = 1.83 μ_B. EPR (toluene, 298 K): g_{iso} = 1.99, A_{iso} = 100 G; (toluene, 10 K) $g_\perp$ = 1.99, $A_\perp$ = 64 G, $g_{||}$ = 1.96, $A_{||}$ = 181 G.

Preparation of [VO(L^{6}H$_2$)$_2$] (9). To a solution of **L^6**H$_3$ (1.00 g, 1.45 mmol) in toluene (30 mL) was added [VO(O-*n*-Pr)$_3$] (0.17 mL, 0.73 mmol). The solution was stirred at room temperature for 4 h after which the solvents were removed in vacuo. The crude material was extracted into cold acetonitrile (40 mL) and filtered giving **9** as brown blocks. Yield: 647 mg, 61%. $C_{92}H_{118}O_7N_4V$ Calcd (found): C, 76.58 (76.46); H, 8.24 (8.35); N, 3.88 (3.82). IR (Nujol mull, cm^{-1}): 3479m, 3335m, 3161m, 2723m, 2671m, 1673m, 1612m, 1592m, 1577m, 1455m, 1376m, 1293m, 1260m, 1191m, 1165m, 1161m, 1094bm, 1018bm, 979m, 884m, 862w, 846w, 801m, 753m, 665m. Magnetic moment: μ = 1.86 μ_B. EPR (toluene, 298 K): g_{iso} = 2.00, A_{iso} = 95 G; (toluene, 10 K) $g_\perp$ = 1.99, $A_\perp$ = 63 G, $g_{||}$ = 1.96, $A_{||}$ = 186 G.

Preparation of [VO(L^{2}H$_2$)$_2$] (10). [V(O)(O-*n*-Pr)$_3$] (0.17 mL, 0.74 mmol) and **L^2**H$_3$ (1.00 g, 1.48 mmol) were refluxed in toluene (40 mL) for 12 h. Upon cooling, the solvents were removed in vacuo, and the brown residue was extracted into dichloromethane (30 mL). Standing at ambient temperature for 24 h afforded **10** as a yellow/brown solid. Yield: 550 mg, 26%. mp: 275 °C (dec). $C_{92}H_{122}N_2O_7V\cdot CH_2Cl_2$ Calcd (found): C, 74.38 (74.58); H, 8.19 (8.29); N, 1.87 (1.75). MS *m*/*z* (EI): 1416 (M$^+$). IR (Nujol mull, cm^{-1}): 3507(m), 3174(m) 1614(m), 1584(m), 1410(m), 1360(m), 1314(w), 1291(w), 1254(m), 1185(m), 1152(m), 1119(m), 1093(m), 1020(m), 977(m), 921(w), 878(w), 799(w), 763(w), 717(w).

Magnetic moment: $\mu = 1.31\ \mu_B$. EPR (toluene, 298 K): $g_{iso} = 2.01$, $A_{iso} = 96$ G; (toluene, 10 K) $g_\perp = 1.99$, $A_\perp = 64$ G, $g_\parallel = 1.95$, $A_\parallel = 185$ G.

Preparation of [VO(L^{3}H$_2$)$_2$] (11). Preparation was done as for **10** but using **L**^{3}H$_3$ (1.00 g, 1.45 mmol) and [V(O)(O-*n*-Pr)$_3$] (0.16 mL, 0.73 mmol), affording **11** as a yellow/green solid. Yield: 430 mg, 20%. mp: 260 °C (dec). $C_{94}H_{126}N_2O_7V$ Calcd (found): C, 78.14 (77.79); H, 8.65 (8.59); N, 1.94 (1.52).MS *m*/*z* (EI): 1444 (M^+). IR (Nujol mull, cm^{-1}): 3530(bm), 3188(bm), 1620(m), 1585(m), 1363(m), 1287(m), 1259(m), 1187(m), 1169(w), 1151(w), 1187(m), 1093(m), 982(w), 874(w), 860(w), 838(w), 802(s), 716(m). Magnetic moment: $\mu = 1.33\ \mu_B$. EPR (toluene, 298 K): $g_{iso} = 1.98$, $A_{iso} = 96$ G; (toluene, 10 K) $g_\perp = 1.99$, $A_\perp = 65$ G, $g_\parallel = 1.95$, $A_\parallel = 185$ G.

Preparation of [VO(L^{4}H$_2$)$_2$] (12). Preparation was done as for **10**, but using **L**^{4}H$_3$(1.00 g, 1.39 mmol) and [V(O)(O-*n*-Pr)$_3$] (0.16 mL, 0.70 mmol) affording **12** as a yellow/brown solid. Yield: 478 mg, 23%. mp: 255 °C (dec). $C_{98}H_{134}N_2O_7V\cdot CH_2Cl_2$ Calcd (found): C, 74.97 (74.64); H, 8.52 (8.74); N, 1.77 (1.54). MS *m*/*z* (EI): 1500 ($M^+ - H$). IR (Nujol mull, cm^{-1}): 3425(bm), 3192(bm), 1611(m), 1586(m), 1255(s), 1187(m), 1151(w), 1118(m), 1090(m), 1011(m), 878(m), 845(m), 795(s), 763(m), 719(m), 662(m). Magnetic moment: $\mu = 1.39\ \mu_B$. EPR (toluene, 298 K): $g_{iso} = 2.01$, $A_{iso} = 96$ G; (toluene, 10 K) $g_\perp = 1.99$, $A_\perp = 65$G, $g_\parallel = 1.96$, $A_\parallel = 180$ G.

Preparation of {(AlMe$_2$)[AlMe(NCMe)]L^1} (13). To a solution of **L**^{1}H$_3$ (1.00 g, 1.32 mmol) in toluene (30 mL) was added 3.1 equiv of trimethylaluminum (2.0 M solution, 2.04 mL, 4.08 mmol). The solution was refluxed overnight, and the solvent was removed in vacuo. Extraction into warm acetonitrile (25 mL) and cooling to ambient temperature gave yellow prisms of **13** (400 mg, 34%). mp: >350 °C. $C_{57}H_{82}N_2O_3Al_2$ Calcd (found): C, 76.3 (76.0); H, 9.2 (9.5); N, 3.1 (2.9). ^{1}H NMR ($CDCl_3$, 400 MHz): δ 8.23 (1H, s, C*H*=N), 7.55−6.98 (9H, m, Ar−*H*), 5.29 (1H, s, Ar$_3$C*H*), 3.00 (2H, m, *i*-Pr), 1.95 (12H, s, *i*-Pr), 1.48−1.22 (45H, overlaying signals, *t*-Bu), 0.07 (3H, s, MeCN), −0.51 (3H, s, Al−C*H*$_3$), −0.81 (3H, s, Al−C*H*$_3$), −1.61 (3H, s, Al−C*H*$_3$). MS *m*/*z* (MALDI): 799 (M − AlMe$_2$ − MeCN). IR (Nujol mull, cm^{-1}): 3131(bm), 1611(s), 1398(m), 1260(m), 1093(m), 1019(m), 858(s), 800(m), 600(s).

Crystallographic Analyses. For each sample, a crystal was mounted in oil on a glass fiber and fixed in the cold nitrogen stream on an automated CCD diffractometer equipped with Mo Kα radiation ($\lambda = 0.71073\ \lambda$) and graphite monochromator, except for compound **6** which was measured at a synchrotron source. In all cases intensity data were measured by thin-slice ω- and φ-scans. Data were processed using the CrysAlis-RED,[44] DENZO/SCALEPACK[45] or SAINT[46] programs. The structures were determined by the direct methods routines in the SHELXS[47] or SIR-92[48] programs and refined by full-matrix least-squares methods, on F^2, in SHELXL.[47] The non-hydrogen atoms were refined with anisotropic thermal parameters, except in some disordered groups and solvent molecules where the partial atoms were refined isotropically. In several compounds, the phenolic hydrogen atoms were located in difference maps and were refined freely; all other hydrogen atoms in all samples were included in idealized positions and their U_{iso} values were set to ride on the U_{eq} values of the parent carbon or nitrogen atoms. Scattering factors for neutral atoms were taken from reference.[49] Crystal data and refinement results are collated in Table 12.

Acknowledgment. The University of East Anglia and the EPSRC are thanked for financial support. We thank the EPSRC Mass Spectrometry Service Centre (Swansea, U.K.). The EPSRC X-ray Crystallography Service, Southampton, U.K., is thanked for data collection of **13**, and the EPSRC is also thanked for the award of beamtime at Daresbury Laboratory (Station 9.8 SMX) and Drs. John Warren and Tim Prior for scientific support. We would also like to thank Rapra Scientific Ltd. for GPC measurements and Dr Myles Cheesman (UEA) for help with recording EPR spectra.

IC702506W

(44) *CrysAlis-CCD* and *-RED*; Oxford Diffraction Ltd.: Abingdon, U.K., 2005.
(45) Otwinowski, Z.; Minor, W. Processing of X-ray diffraction data collected in the oscillation mode. *Macromolecular Crystallography, Part A*; Methods in Enzymology 276; Carter, C. W., Jr., Sweet, R. M., Eds.; Academic Press: San Diego, CA. , 1997; pp 307−326.
(46) *SAINT software for CCD diffractometers*, Bruker AXS, Inc., Madison, WI, 2001.
(47) Sheldrick, G. M. *Acta Crystallogr.* **2008**, *A64*, 112–122.
(48) Altomare, A.; Cascarano, G.; Giacovazzo, C.; Guagliadi, A. *J. Appl. Crystallogr.* **1993**, *26*, 343.
(49) *International Tables for X-ray Crystallography*; Kluwer Academic Publishers: Dordrecht, The Netherlands, 1992; Vol C, pp. 500, 219, 193.